

# Lepton number violating mSUGRA and neutrino masses

---

**B.C. Allanach and C.H. Kom**

*DAMTP, Centre for Mathematical Sciences,  
Wilberforce Road, Cambridge, CB3 0WA, U.K.*

*E-mail: b.c.allanach@damtp.cam.ac.uk, c.kom@damtp.cam.ac.uk*

**ABSTRACT:** We perform a quantitative study of neutrino phenomenology in the framework of minimal supergravity (mSUGRA) with grand unified theory (GUT)-scale tri-linear lepton number violation. We show that only two non-zero GUT scale lepton number violating parameters and three charged lepton mixing angles are sufficient to account for current neutrino oscillation data. This allows collider studies to be performed in a manageable parameter space. We discuss some phenomenological consequences of the models, including tuning issues.

**KEYWORDS:** Supersymmetry Phenomenology, Neutrino Physics.

---

## Contents

<b>1. Introduction</b>	<b>1</b>
<b>2. Neutrino masses and mixings</b>	<b>4</b>
<b>3. Numerical procedure</b>	<b>13</b>
<b>4. Results</b>	<b>16</b>
<b>5. Discussion</b>	<b>23</b>
<b>A. Mass matrices</b>	<b>25</b>
<b>B. One loop self energies of the neutral fermions</b>	<b>28</b>
<b>C. Mass insertion approximation in CPE-CPO cancellations</b>	<b>29</b>
<b>D. Calculation of <math>l^I \rightarrow l^J \gamma</math></b>	<b>31</b>

---

## 1. Introduction

In general, the minimal supersymmetric standard model (MSSM) contains baryon and lepton number violating (LNV) operators in the superpotential [1]. This generally leads to fast proton decay beyond experimental limits, unless an additional symmetry is imposed on the theory. The most widely studied symmetry is R-parity, which forbids all problematic renormalisable operators and makes the lightest supersymmetric particle (LSP) stable, providing a potential dark matter candidate. However, there are still dimension five operators which may be dangerous for proton decay [2]. If one instead imposes an anomaly-free proton hexality discrete abelian symmetry  $P_6$  [3], such dimension five operators are forbidden. Another alternative to ensure slow enough proton decay is so-called baryon triality, which is an anomaly-free  $\mathcal{Z}_3$  symmetry [4] and forbids baryon number violating terms past dimension five. The model allows a subset of all available MSSM R-parity violating operators [5], namely the LNV operators. LNV operators in turn lead to the generation of neutrino masses. Thus, the LNV MSSM provides an alternative neutrino mass generation mechanism to the see-saw mechanism [6, 7], in which gauge singlet right-handed neutrino superfields are added to the  $P_6$ -conserving MSSM. Although the LSP becomes unstable in such schemes, it could still form a dark matter candidate if it is the gravitino, since the decays are slow on cosmological time scales [8]. Here, we shall neglect the dark matter relic density, since it could instead originate from a hidden sector. The aim of this paper

is to find and investigate simple GUT-scale LNV MSSM models that can give rise to the observed neutrino mass and mixing pattern.

The chiral superfields of the MSSM are charged under the standard model (SM) gauge group  $G_{\text{SM}} = \text{SU}(3)_c \otimes \text{SU}(2)_L \otimes \text{U}(1)_Y$  as

$$\begin{aligned} Q &: (3, 2, \frac{1}{6}), & \bar{U} &: (\bar{3}, 1, -\frac{2}{3}), & \bar{D} &: (\bar{3}, 1, \frac{1}{3}), \\ L &: (1, 2, -\frac{1}{2}), & H_d &: (1, 2, -\frac{1}{2}), \\ \bar{E} &: (1, 1, 1), & H_u &: (1, 2, \frac{1}{2}). \end{aligned} \tag{1.1}$$

The full renormalisable LNV MSSM superpotential is given by

$$\mathcal{W} = \mathcal{W}_{\text{RPC}} + \mathcal{W}_{\text{LNV}}, \tag{1.2}$$

where  $\mathcal{W}_{\text{RPC}}$  is the superpotential in the R-parity conserving (RPC) case, and  $\mathcal{W}_{\text{LNV}}$  is the LNV superpotential given by

$$\begin{aligned} \mathcal{W}_{\text{RPC}} &= (Y_E)_{ij} H_d L_i \bar{E}_j + (Y_D)_{ij} H_d Q_i \bar{D}_j + (Y_U)_{ij} Q_i H_u \bar{U}_j - \mu H_d H_u, \\ \mathcal{W}_{\text{LNV}} &= \frac{1}{2} \lambda_{ijk} L_i L_j \bar{E}_k + \lambda'_{ijk} L_i Q_j \bar{D}_k - \mu_i L_i H_u, \end{aligned} \tag{1.3}$$

where we have suppressed gauge indices and  $\{i, j, k\} \in \{1, 2, 3\}$  are family indices.  $(Y_E)$ ,  $(Y_D)$  and  $(Y_U)$  are  $3 \times 3$  matrices of dimensionless Yukawa couplings;  $\lambda_{ijk}$ ,  $\lambda'_{ijk}$  are the dimensionless tri-linear LNV couplings, and  $\mu_i$  are dimensionful bi-linear LNV parameters. The soft supersymmetry (SUSY) breaking Lagrangian with LNV is given by

$$-\mathcal{L}_{\text{soft}} = \mathcal{L}_{\text{RPC}}^{\text{mass}} + \mathcal{L}_{\text{RPC}}^{\text{int}} + \mathcal{L}_{\text{LNV}}, \tag{1.4}$$

where

$$\begin{aligned} \mathcal{L}_{\text{RPC}}^{\text{mass}} &= \frac{1}{2} M_1 \tilde{B} \tilde{B} + \frac{1}{2} M_2 \tilde{W} \tilde{W} + \frac{1}{2} M_3 \tilde{g} \tilde{g} + h.c. \\ &+ \tilde{Q}^\dagger \left( m_{\tilde{Q}}^2 \right) \tilde{Q} + \tilde{U}^\dagger \left( m_{\tilde{U}}^2 \right) \tilde{U} + \tilde{D}^\dagger \left( m_{\tilde{D}}^2 \right) \tilde{D} + \tilde{L}^\dagger \left( m_{\tilde{L}}^2 \right) \tilde{L} + \tilde{E}^\dagger \left( m_{\tilde{E}}^2 \right) \tilde{E} \\ &+ m_{h_u}^2 h_u^\dagger h_u + m_{h_d}^2 h_d^\dagger h_d, \\ \mathcal{L}_{\text{RPC}}^{\text{int}} &= (h_E)_{ij} h_d \tilde{L}_i \tilde{E}_j + (h_D)_{ij} h_d \tilde{Q}_i \tilde{D}_j + (h_U)_{ij} \tilde{Q}_i h_u \tilde{U}_j - \tilde{B} h_d h_u + h.c., \\ \mathcal{L}_{\text{LNV}} &= \frac{1}{2} h_{ijk} \tilde{L}_i \tilde{L}_j \tilde{E}_k + h'_{ijk} \tilde{L}_i \tilde{Q}_j \tilde{D}_k - \tilde{D}_i \tilde{L}_i h_u \\ &+ h_d^\dagger m_{H_d L_i}^2 \tilde{L}_i + h.c. \end{aligned} \tag{1.5}$$

where tilde denotes a super-partner of the more familiar Standard Model field.  $M_1$ ,  $M_2$  and  $M_3$  are the masses of the super-partner of the SM gauge bosons, the  $m^2$ 's are the scalar mass parameters of the sparticle and/or higgs fields, and the  $h$ 's,  $\tilde{B}$  and  $\tilde{D}_i$  are trilinear SUSY breaking parameters that correspond to the dimensionless supersymmetric parameters displayed in eq. (1.3). Tree level neutrino masses originating from such a theory were derived in refs. [10, 9]. Some of the weak-scale parameters in eqs. (1.3), (1.5) were bounded by neutrino oscillation data in refs. [11, 12]. The bi-linear couplings have been employed to fit solar and atmospheric neutrino oscillations at the weak scale [13–15]. Work on bi-linear

couplings in the MSSM can also be found in refs. [16–18]. Early attempts to calculate tri-linear coupling contributions to the neutrino masses can be found in [19–23]. A basis independent calculation was performed in [24]. The complete set of 1-loop corrections to neutrino masses and mixings were investigated in detail in [25]. There, collections of weak-scale couplings that could give rise to the tri-bi maximal mixing pattern [26] were suggested. Such a pattern provides a successful fit to oscillation constraints on lepton mixing.

The number of parameters in eq. (1.5) may be reduced by assumptions about the structure and origin of the supersymmetry breaking terms. We take the concrete example of the mSUGRA assumption,<sup>1</sup> where at a high energy GUT scale  $M_X \sim 10^{16}$  GeV the scalar masses are set to be diagonal and equal to  $m_0$ , all soft trilinear couplings are equal to their analogous superpotential parameter multiplied by a common coupling  $A_0$  and all gaugino masses are set to be equal to  $M_{1/2}$ . Constraints upon such a model including LNV effects have been studied in refs. [27, 28]. In the latter, a cosmological bound  $\sum_i m_{\nu_i} < 0.7$  eV was placed upon the model but no attempt was made to fit the neutrino properties deduced from oscillation measurements. In ref. [29], three relatively large  $\lambda'_{ijk}$  defined in a weak basis at the GUT scale were used to generate  $\kappa_i$  and  $\lambda'_{i33}$  at the weak scale. These couplings are required to satisfy upper bounds obtained from neutrino oscillation data. The input parameters are not directly related to neutrino phenomenology, but lead to interesting collider signals. However, no detailed fitting of the neutrino oscillation data was attempted. Bi-linear contributions to the neutrino masses in LNV mSUGRA were considered in ref. [30]. Solutions with 3 non-zero GUT scale LNV parameters  $\mu_i$  were found. Also, a preference for the vacuum oscillation solution [31] to the solar neutrino problem was stated. This has since been ruled out by KamLAND data [32]. An attempt to fit the neutrino masses in LNV mSUGRA using  $\lambda_{i33}$  and  $\lambda'_{i33}$  in the charged lepton mass basis was made in ref. [33] using the renormalization group equations (RGEs) of ref. [34]. Only the atmospheric mixing angle and the neutrino mass squared differences were included in the fit and a preference towards the small mixing angle MSW [35] solution for the solar neutrinos was found. The latter has also been excluded by KamLAND, which favours the large angle MSW region of parameter space.

In the present paper, we shall follow an alternative approach. At the GUT scale and in the weak interaction basis where all soft terms are diagonal in flavour space, we shall assume zero bi-linear LNV operators. In this basis, we shall introduce a small number of non-zero tri-linear LNV operators, following ref. [28]. Further non-zero bi- and tri-linear couplings are generated on renormalisation to the weak scale. One may hope that a single GUT-scale tri-linear operator could then be enough to generate neutrino masses. We shall find that a single non-zero trilinear coupling is insufficient to reproduce the neutrino mass pattern observed. A further operator shall be necessary. Although we assume only two non-zero LNV couplings, we think of this only as a limiting case, where any other LNV parameters contribute negligibly to the neutrino masses and hence are neglected. Such flavour structure may arise from some fundamental flavour physics models which yield a small number of dominant LNV couplings in the weak interaction basis, mirroring the case

---

<sup>1</sup>Also termed the constrained MSSM.

of the Standard Model Yukawa couplings.

The paper proceeds as follows: section 2 explains the difficulty in obtaining the observed neutrino mass hierarchy with only one R-parity violating (RPV)<sup>2</sup> parameter at  $M_X$  in any flavour basis, and suggests how the next to minimal case with two RPV parameters (defined in a mixed charged lepton basis) may get around the problems. We then describe a numerical procedure to find the best fit value for the 2 RPV parameters, as well as the 3 mixing angles which define the mixed charged lepton basis in section 3. The results are presented in section 4, where we briefly speculate about possible collider signatures. We compare our paper with selected work in the literature, and discuss issues related to parameter tuning before concluding in section 5. We set our notation in appendix A, and the general expressions for the 1-loop neutrino-neutralino mass corrections in appendix B. Appendix C describes the mass insertion approximation for CP even and CP odd neutral scalar contributions (required for numerical stability), and finally in appendix D a full calculation of the branching ratio of  $l^I \rightarrow l^J \gamma$  is presented, which will be used to constrain the LNV parameters.

## 2. Neutrino masses and mixings

In a recent global 3 neutrino fit to all oscillation data [36], the following ranges of parameters at  $1\sigma$  were found

$$\begin{aligned} \Delta m_{21}^2 &= 7.9_{-0.28}^{+0.27} \times 10^{-5} \text{eV}^2, & |\Delta m_{31}^2| &= 2.6 \pm 0.2 \times 10^{-3} \text{eV}^2, & (2.1) \\ \sin^2 \theta_{12} &= 0.31 \pm 0.02, & \sin^2 \theta_{23} &= 0.47_{-0.07}^{+0.08}, & \sin^2 \theta_{13} &= 0_{-0.0}^{+0.008}. \end{aligned}$$

Here  $\Delta m_{21}^2$  and  $\Delta m_{31}^2$  denote the mass squared differences between the three neutrinos responsible for solar and atmospheric oscillations respectively. The  $\sin^2 \theta$ 's represent the rotation angles characterizing the PMNS matrix [37], the lepton counterpart to the CKM matrix, in the standard parameterization [38]. First, we shall discuss some issues concerning mixing matrices and effective neutrino and charged lepton mass matrices in the presence of lepton number violation.

Since we work in the weak interaction basis, it is instructive to understand how diagonalization of the charged lepton Yukawa matrix behaves, particularly under renormalization. In the R-parity conserving limit and in the absence of the neutrino Yukawa matrix, one can simply rotate the leptonic superfields back to a basis where all the leptonic terms are flavour diagonal at  $M_X$ . The rotation matrices  $Z_{lL}$  and  $Z_{lR}$  are defined by

$$Z_{lL}^\dagger Y_E Z_{lR} = \hat{Y}_E, \tag{2.2}$$

where  $\hat{Y}_E$  is diagonal. Since mSUGRA soft terms are diagonal in flavour space, there is no intrinsic flavour violation in the RPC limit. It is therefore always possible to diagonalise the leptonic Yukawa couplings and the slepton mass matrix by the same rotations even after renormalization to lower scales. The rotation is also renormalization scale independent.

---

<sup>2</sup>We will use RPV and LNV interchangeably in this paper.

To show this we examine the renormalization group (RG) equations of  $Y_E$  [39], keeping only terms proportional to Yukawa matrices, as the gauge coupling contributions are flavour blind and so cannot change the lepton mixing. At 1-loop, we have

$$\begin{aligned} \frac{d}{dt} Y_E &= \frac{1}{(4\pi)^2} Y_E \{ \text{Tr}(3Y_D Y_D^\dagger + Y_E Y_E^\dagger) + 3Y_E^\dagger Y_E + \text{g.c.} \} \\ &\equiv a Y_E \left\{ Y_E^\dagger Y_E + \hat{\beta} \left( \text{Tr} \left( Y_D Y_D^\dagger \right), \text{Tr} \left( Y_E Y_E^\dagger \right), g_1, g_2 \right) \right\}, \end{aligned} \quad (2.3)$$

where g.c. stands for gauge contributions and  $t = \ln \mu$  is the natural logarithm of the  $\overline{DR}$  renormalisation scale. The function  $\hat{\beta}(\text{Tr}(Y_D Y_D^\dagger), \text{Tr}(Y_E Y_E^\dagger), g_1, g_2)$  depends on the trace of the quark and lepton Yukawa matrices as well as the gauge couplings, and so is proportional to the unit matrix and do not change lepton flavours as a result.

Writing  $Y_E(t) \equiv Y_t$ ,  $\hat{\beta}(t) \equiv \hat{\beta}_t$  and  $Y_E(0) = Y_0$ , we obtain

$$Y_t = Y_0 + a \int_0^t dt_1 Y_{t_1} \left( Y_{t_1}^\dagger Y_{t_1} + \hat{\beta}_{t_1} \right). \quad (2.4)$$

We may then plug eq. (2.4) back into itself in order to obtain an expansion

$$\begin{aligned} Y_t &= Y_0 + a \int_0^t dt_1 \left[ Y_0 + a \int_0^{t_1} dt_2 Y_{t_2} \left( Y_{t_2}^\dagger Y_{t_2} + \hat{\beta}_{t_2} \right) \right] \\ &\quad \left\{ \left[ Y_0 + a \int_0^{t_1} dt_2 Y_{t_2} \left( Y_{t_2}^\dagger Y_{t_2} + \hat{\beta}_{t_2} \right) \right]^\dagger \left[ Y_0 + a \int_0^{t_1} dt_2 Y_{t_2} \left( Y_{t_2}^\dagger Y_{t_2} + \hat{\beta}_{t_2} \right) \right] + \hat{\beta}_{t_1} \right\}. \end{aligned} \quad (2.5)$$

Eq. (2.4) may be substituted back into eq. (2.5) an arbitrary number of times, but it is clear that all terms are products of terms which are either of the form  $\int dt_n Y_{t_n} (Y_{t_n}^\dagger Y_{t_n}) D(t_n)$  or  $\int dt_n Y_{t_n} D'(t_n)$  where  $D(t_n)$  and  $D'(t_n)$  are some functions of  $t_n$  which are diagonal in flavour space. We may now calculate  $Y_t$  to arbitrary order in  $a$ , for example

$$Y_t = Y_0 + a \left[ A Y_0 + t Y_0 Y_0^\dagger Y_0 \right] + a^2 \left[ \frac{3t^2}{2} Y_0 Y_0^\dagger Y_0 Y_0^\dagger Y_0 + B Y_0 Y_0^\dagger Y_0 + C Y_0 \right] + \mathcal{O}(a^3), \quad (2.6)$$

where  $A = \int_0^t dt_1 \hat{\beta}_{t_1}$ ,  $B = 3 \int_0^t dt_1 \int_0^{t_1} dt_2 \hat{\beta}_{t_2} + \int_0^t dt_1 t_1 \hat{\beta}_{t_1}$  and  $C = \int_0^t dt_1 \hat{\beta}_{t_1} \int_0^{t_1} dt_2 \hat{\beta}_{t_2}$ . It is clear that higher order corrections always have the form  $Y_0 (Y_0^\dagger Y_0)^n$  plus some diagonal piece, and so both  $Y_t$  and  $Y_0$  can be diagonalized by the same mixing matrices  $Z_{lL(R)}$ . This procedure can be generalised to higher loops, but we decline to do so here. Intuitively, in a non-diagonal  $Y_E$  basis, the mass eigenstates are defined by the vectors in the lepton mixing matrices  $Z_{lL}$  and  $Z_{lR}$ , and after the rotation the new flavour basis coincides with the mass basis. Because there is no intrinsic lepton flavour changing physics in the Lagrangian, these mass eigenstates cannot mix with each other under renormalization, except through a trace which then affects all three flavours in the same way. The mixing matrices hence remain the same.

This means that even though we work in a non-diagonal lepton flavour basis, lepton flavour changing processes only arise from the LNV couplings and are suppressed by even powers of them since the LNV operators violate lepton number by one unit and the Majorana neutrino masses generated violate it by two. Another source of leptonic flavour

changing neutral current (FCNC) would arise when one allows for non-universal SUSY breaking boundary conditions, which is common in unified model building. This is a separate issue and has been discussed extensively in the literature, see e.g. [40].

The LNV operators also make the rotation matrices  $Z_{lL}$  and  $Z_{lR}$  scale dependent. However as R-parity violation is small in our analysis, the mixing matrices are scale independent to a very good approximation. For numerical convenience, we rotate to a diagonal charged lepton Yukawa matrix basis at  $M_X$  before renormalizing down to  $M_Z$ . In general this means that there are a lot of LNV parameters in the diagonal basis, however they are all related to each other by the rotation.

We will first investigate the case with one non-zero dimensionless LNV coupling at  $M_X$ , and then go on to discuss the case of 2 non-zero LNV parameters. The RG evolution will dynamically generate all LNV parameters allowed by symmetry. This includes the dimensionful  $\mu_i$ 's, which implies non-zero sneutrino vacuum expectation values (vev) upon minimizing the Higgs-sneutrino potential [28]. These effects are important in determining the neutrino mass pattern and will be described in detail in the following sections. The mass matrices used to compute the radiative corrections of the neutrinos and neutralinos are presented in appendix A and references therein.

The tree level,  $7 \times 7$  neutrino-neutralino mass matrix  $\mathcal{M}_N$  generates an effective  $3 \times 3$  neutrino mass matrix through a seesaw mechanism. Writing  $\mathcal{M}_N$  as defined in appendix A,

$$\mathcal{M}_N = \begin{pmatrix} \mathcal{M}_{\chi^0} & m^T \\ m & m_\nu \end{pmatrix}, \quad (2.7)$$

where  $m_\nu$  and  $m$  contain the lepton number violating contributions, and  $\mathcal{M}_{\chi^0}$  is the neutralino mass matrix which plays the suppression role of the right handed heavy neutrinos in the standard see-saw mechanism [7]. The effective mass matrix  $\mathcal{M}_{\text{eff}}^\nu$  is then given by

$$\mathcal{M}_{\text{eff}}^\nu = m_\nu - m \mathcal{M}_{\chi^0}^{-1} m^T. \quad (2.8)$$

At tree level,  $m_\nu = 0_{3 \times 3}$  and the effective mass matrix is given by [10, 9]

$$\mathcal{M}_{\text{eff}}^\nu = \frac{(M_1 g_2^2 + M_2 g^2)}{2\mu[v_u v_d (M_1 g_2^2 + M_2 g^2) - \mu M_1 M_2]} \begin{pmatrix} \Lambda_e \Lambda_e & \Lambda_e \Lambda_\mu & \Lambda_e \Lambda_\tau \\ \Lambda_\mu \Lambda_e & \Lambda_\mu \Lambda_\mu & \Lambda_\mu \Lambda_\tau \\ \Lambda_\tau \Lambda_e & \Lambda_\tau \Lambda_\mu & \Lambda_\tau \Lambda_\tau \end{pmatrix}. \quad (2.9)$$

$g_2, g$  are the SU(2) and U(1)<sub>Y</sub> gauge couplings, and  $v_u, v_d$  are the vacuum expectation values (vevs) of the neutral components of  $H_u, H_d$  respectively. Also,

$$\Lambda_i \equiv \mu v_i - v_d \mu_i, \quad i = \{e, \mu, \tau\}, \quad (2.10)$$

and so  $\mathcal{M}_{\text{eff}}^\nu$  depends on the sneutrino vevs  $v_i$  and LNV supersymmetric bilinear parameters  $\mu_i$ .  $\mathcal{M}_{\text{eff}}^\nu$  is of rank 1, so there is one non-zero eigenvalue

$$m_{\text{heavy}} = \frac{(M_1 g_2^2 + M_2 g^2) \sum_i \Lambda_i^2}{2\mu [v_u v_d (M_1 g_2^2 + M_2 g^2) - \mu M_1 M_2]}. \quad (2.11)$$

Clearly this is not compatible with the experimentally measured mass squares differences, which require at least two non-zero neutrino masses. Including one-loop contributions can give mass to the other neutrinos. In the rest of this work we will present a minimal construction in which the observed mass pattern can be obtained.

The complete one-loop self-energies for the neutralinos and neutrinos in 2 component notation, including all terms with R-parity violation are given in [25]. Here we present the general expression in a matrix form compatible with the notation of [41]. The one-loop corrected neutrino-neutralino mass matrix  $\mathcal{M}'_N$  is given by

$$(\mathcal{M}'_N)_{ij} = (\mathcal{M}_N)_{ij} + \frac{1}{2} (\delta\mathcal{M} + \delta\mathcal{M}^T)_{ij}, \quad (2.12)$$

where

$$\delta\mathcal{M}_{ij} = (\Sigma_D)_{ij} - (\mathcal{M}_N)_{ik}(\Sigma_L)_{kj}, \quad (2.13)$$

and  $\Sigma_D$  and  $\Sigma_L$  are mass corrections and wavefunction renormalization respectively.

As in [41], we perform the full renormalization with external legs in a flavour basis. The Feynman rules including all LNV terms can be obtained in the appendix of [25], and by rotating one external neutral fermion leg from mass basis into flavour basis. The physical masses are obtained by diagonalising  $\mathcal{M}'_N$ .

Upon diagonalising  $\mathcal{M}'_N$ , a  $7 \times 7$  mixing matrix  $Z'_N$  is obtained. As at tree level, one may also obtain an effective neutrino mass matrix  $\mathcal{M}'_{\text{eff}}{}^\nu$  using eq. (2.8). In particular, the  $3 \times 3$  sub-matrix  $m_\nu$  receives radiative contributions and plays a significant role in determining the effective neutrino mass matrix. The mixing between the neutrinos and the neutralinos is suppressed by the smallness of the LNV couplings and  $v_i$  with respect to the other neutralino matrix parameters, and is neglected for the purpose of calculating the PMNS matrix. The neutrino mixing matrix  $Z_\nu$  is then defined by

$$Z_\nu^T \mathcal{M}'_{\text{eff}}{}^\nu Z_\nu = \text{diag}[m_i], \quad i = 1, 2, 3. \quad (2.14)$$

The charged lepton-chargino mass matrix is treated similarly, where one can again use a see-saw mechanism to obtain an effective mass matrix with the charginos providing the see-saw suppression. In this case however, the see saw contribution to the effective mass matrix is suppressed by two powers of LNV parameters, and is negligible compared with  $Y_E$ . So for the purpose of calculating the charged lepton mixing matrix, one can simply use  $Y_E$  and hence the same  $Z_{lL}$  and  $Z_{lR}$  as before. After rotating to a basis with diagonal lepton Yukawa couplings at  $M_X$ , the lepton *flavour* changing terms in the Yukawa matrix  $Y_E$  are generated by terms at least quadratic in  $\lambda$  by the RG evolution, and again such contributions are neglected when calculating the PMNS matrix.

The observable PMNS mixing matrix which connects the charged lepton and neutrino



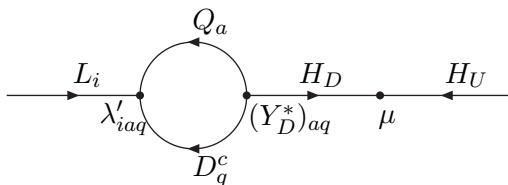


**Figure 1:** Dynamical generation of  $\mu_i$ .

mass eigenstates is defined by<sup>3</sup>

$$U_{\text{PMNS}} = Z_{1L}^T Z_\nu, \quad (2.15)$$

where  $Z_{1L}$  is the mixing matrix of the left handed charged leptons. In the present paper, we always work in the CP-conserving limit and thus  $Z_{1L}^\dagger = Z_{1L}^T$ . Because we are already working in a basis where the charged lepton mass matrix is practically diagonal, the PMNS matrix is the same as  $Z_\nu$ , and they will be used inter-changeably in the rest of the paper.

### The ratio of tree level to loop level mass scales

It is well known that even if the high scale theory has all bilinear LNV couplings set to zero, the RG flow will dynamically generate  $\mu_i$ ,  $\tilde{D}_i$  and  $m_{H_d L_i}^2$  at low scale, and hence  $v_i$  after minimizing the higgs-sneutrino scalar potential. These effects are important, because the dimensionless LNV couplings contribute to the effective neutrino mass matrix at both loop level and tree level in a related way. Typically the tree level mass scale dominates over the loop contributions, despite the fact that the bilinear parameters themselves are originated from radiative corrections. Also, the loop induced mass matrix tends to align with (i.e. is proportional to) the tree level mass matrix, further suppressing radiatively induced neutrino masses.

With only one trilinear LNV parameter in the diagonal charged lepton basis, the above statements are generally true. However one LNV parameter in the weak interaction basis corresponds to many LNV couplings in a diagonal charged lepton basis, related by the charged lepton mixings. These rotations need not be small because the observed PMNS mixings are near tri-bi maximal, so we may expect a ‘democratic’ distribution of LNV couplings. However the fact that these parameters are related implies that both the alignment effect and the hierarchy between the tree and loop mass scale persists. We will show how this happens in the following, and then go on to discuss the next minimal case of two LNV operators (in the weak interaction basis).

---

<sup>3</sup>Note in 4 component Dirac notation, the  $Y_E$  is typically associated with the term  $\bar{L}_L Y_E E_R h_d$  in other conventions. This  $Y_E$  is the *complex conjugate* of the  $Y_E$  that appears in the superpotential in eq. (1.3). This is why we have  $U_{\text{PMNS}} = Z_{1L}^T Z_\nu$  instead of  $U_{\text{PMNS}} = Z_{1L}^\dagger Z_\nu$ . However our numerical calculation assumes CP conservation, so the two are equivalent. The results presented in this paper follow the convention defined by eq. (1.3), and we keep track of the complex conjugations for book keeping purposes.

In scenarios with R-parity violation dominated by one  $\lambda$ , one can approximate the tree level mass scale by [28] (see also [42])<sup>4</sup>

$$m_\nu^{\text{tree}} \simeq -\frac{8\pi\alpha_{\text{GUT}}}{5M_{1/2}} \left[ \frac{v_d}{16\pi^2} \right]^2 \left[ \ln \frac{M_X}{M_Z} \right]^2 [\lambda_{ijq}(Y_E^*)_{jq}]^2 f^2 \left( \frac{\mu^2}{m_0^2}; \frac{A_0^2}{m_0^2}; \frac{\tilde{B}}{m_0^2}; \tan\beta \right), \quad (2.16)$$

where  $f$  is a dimensionless function of  $\mathcal{O}(10)$ . To understand the form of this expression, note that the tree level neutrino mass is obtained by  $\Lambda_i$  in eq. (2.10), which is proportional to  $\mu_i$  and the sneutrino vevs  $v_i$ , while the latter also scale like  $\mu_i$  up to effects from the Yukawa couplings. The dynamical generation of  $\mu_i$ , neglecting sub-dominant terms proportional to  $\mu_i$  itself, is determined by the RG flow

$$16\pi^2 \frac{d}{dt} \mu_i = -\mu(\lambda_{ijk}(Y_E^*)_{jk} + 3\lambda'_{ijk}(Y_D^*)_{jk}), \quad (2.17)$$

so a first estimate of  $\mu_i$  at  $M_Z$  may be obtained by naively integrating the right hand side of the above equation, yielding

$$\mu_i = \frac{1}{(4\pi)^2} \ln \left( \frac{M_X}{M_Z} \right) (\lambda_{ijk}(Y_E^*)_{jk} + 3\lambda'_{ijk}(Y_D^*)_{jk}) \mu + \mathcal{O} \left( \frac{1}{(4\pi)^4} \ln^2 \frac{M_X}{M_Z} \right). \quad (2.18)$$

A pseudo-Feynman diagram in terms of superfields for the second term of eq. (2.18) is shown in figure 1.

On the other hand, the scale of the radiative corrections can be approximated by the part of  $\Sigma_D$  in eq. (2.13) which correspond to  $m_\nu$  in eq. (2.8) (see also [25]). We define this scale to be

$$m_\nu^{\text{loop}} \equiv \sum_{i=1}^3 (\Sigma_{Dii}) \simeq 2 \sum_{i,j,k} \lambda_{iL_j R_k} \lambda_{iL_k R_j} \frac{m_{f_j}^*}{(4\pi)^2} \frac{(\mathcal{M}_{\tilde{f}}^{2*})_{L_k R_k}}{(\mathcal{M}_{\tilde{f}}^2)_{L_k L_k} - (\mathcal{M}_{\tilde{f}}^2)_{R_k R_k}} \ln \frac{(\mathcal{M}_{\tilde{f}}^2)_{L_k L_k}}{(\mathcal{M}_{\tilde{f}}^2)_{R_k R_k}}, \quad (2.19)$$

where the summation  $i$  is over external neutrino flavour eigenstates in the basis defined in appendix A.  $m_{f_j}^*$ <sup>5</sup> is the chirality flip of the fermion propagator with legs labelled by  $L_j$  and  $R_j$ , and the  $\mathcal{M}^2$ 's represent mass insertions with appropriate scalar ‘handedness’. A mass insertion diagram of  $m_\nu^{\text{loop}}$  is displayed in figure 2. The factor of 2 on the right hand side of eq. (2.19) accounts for the set of loop diagrams in figure 2 with the scalar and fermion propagators interchanged. The approximation for  $\lambda'$  is exactly the same, apart from extra colour factors  $n_c = 3$  for both eq. (2.16) and eq. (2.19).

The ratio  $m_\nu^{\text{tree}}/m_\nu^{\text{loop}}$  can then be approximated to be

$$\frac{m_\nu^{\text{tree}}}{m_\nu^{\text{loop}}} \simeq -n_c \frac{\alpha_{\text{GUT}} \ln^2(M_X/M_Z)}{10\pi M_{1/2}(A_0 - \mu \tan\beta)} \frac{(\mathcal{M}_{\tilde{f}}^2)_{L_k L_k} - (\mathcal{M}_{\tilde{f}}^2)_{R_k R_k}}{\ln \left( \frac{(\mathcal{M}_{\tilde{f}}^2)_{L_k L_k}}{(\mathcal{M}_{\tilde{f}}^2)_{R_k R_k}} \right)} f^2 \left( \frac{\mu^2}{m_0^2}; \frac{A_0^2}{m_0^2}; \frac{\tilde{B}}{m_0^2}; \tan\beta \right), \quad (2.20)$$

<sup>4</sup>Note that the normalization of the higgs vev in the current paper is different from [28]. See appendix A.

<sup>5</sup>The phases of the charged lepton mass matrix  $m_f$  can always be rotated away by redefinition of the lepton fields. However we find leaving the redundant complex conjugations helpful when considering chirality flips in loop diagrams.

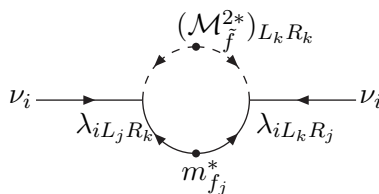


**Figure 2:** A mass insertion diagram which represents the loop corrections to  $m_\nu^{\text{loop}}$  by  $\lambda_{iL_j R_k}$  and  $\lambda_{iL_k R_j}$ .

where we have made the approximation

$$(\mathcal{M}_{\tilde{f}}^2)_{L_k R_k} \sim m_{f_k}(A_0 - \mu \tan\beta), \tag{2.21}$$

where  $\tilde{f}$  represents sleptons or squarks, as appropriate. Setting  $\alpha_{\text{GUT}} = 0.041$  and  $M_X = 10^{16}$  GeV, a rough scan along the SPS1 slope [43] with  $M_{1/2} = [250, 750]$  and also  $\tan\beta = [10, 40]$  gives  $m_\nu^{\text{tree}}/m_\nu^{\text{loop}}$  of order  $\mathcal{O}(30-80)$  for  $\lambda_{ijj}$ , and  $\mathcal{O}(70-200)$  for  $\lambda'_{ijj}$ , in agreement with the approximation of eq. (2.20). However, this is too large to account for the mild empirical neutrino mass hierarchy of a factor of  $\lesssim 6$  from eq. (2.1), assuming negligible lightest neutrino mass.<sup>6</sup>

Note that in the above discussion, alignment (proportionality) between the tree level neutrino effective mass matrix and the radiative correction has not yet been included. The inclusion of such effects will enhance the hierarchy between the heavy and the light neutrino masses obtained in the above approximation. Because at tree level there is only one massive neutrino, exact alignment would imply still only one massive neutrino after the inclusion of radiative corrections. Misalignment between the tree level contributions and the radiative corrections will give rise to light neutrino masses. The size of the mass prediction for the second lightest neutrino compared to the heaviest neutrino, and hence  $|\Delta m_{21}^2|$  compared to  $|\Delta m_{31}^2|$ , can be estimated by the amount of misalignment, multiplied by the ratio of the loop/tree level scales.

To discuss possible alignment effects, it is instructive to first start in the charged lepton mass basis with one LNV coupling. In the latter case, if the LNV coupling violates only one lepton flavour, then the other two lepton flavours are separately conserved. Each of the tree level and loop level neutrino mass matrices can only have one non-zero entry corresponding to the lepton flavour violated, and so these contributions to the full neutrino mass matrix are exactly aligned. Using this flavour symmetry argument it is easy to see that this alignment will persist to all orders in perturbation theory. On the other hand, if the LNV coupling violates all three lepton flavours, then no bilinear LNV couplings can be dynamically generated. There is no source which violates lepton flavour by two units, therefore we cannot generate a one-flavour violating bilinear term from a three-flavour violating term. This can be seen explicitly in the one-loop approximation by reference to eq. (2.17). Thus no tree level mass matrix can be generated. The same reasoning, together

---

<sup>6</sup>In the opposite extreme of a quasi-degenerate mass spectrum, there is clearly no mass ‘hierarchy’.

with the requirement of an odd number of chirality flips in the loop diagrams, also implies that the radiative correction to the neutrino mass matrix is zero.

When the one LNV coupling is defined in the weak interaction basis, which need not coincide with the diagonal charged lepton basis, exact alignment will cease to hold, as the above symmetry arguments do not apply any more. However, it is possible to show that to lowest order in perturbation theory, there is still alignment between the tree level and loop level contributions. For this purpose, we work in a diagonal lepton basis, and make use of the fact that in the R-parity conserving limit, the mixing matrices that rotate into the diagonal basis obey

$$Z_{lL} = Z_{\hat{l}L} \quad Z_{lR} = Z_{\hat{l}R} \quad (\mathcal{M}_l^2)_{L_j R_k} \propto (Y_E)_{L_j R_k}. \quad (2.22)$$

Eq. (2.22) is true at all renormalization scales, as discussed in the previous section with universal boundary conditions due to the absence of intrinsic lepton flavour violation. The universality of the lepton and slepton mixings will be violated at order  $\lambda^2$ , but we shall study small values ( $\lesssim 10^{-3}$ ) of  $\lambda$  and so the non-universality is neglected in our lowest order approximation. We will also make use of the fact that all dynamically generated LNV couplings are small, as will be seen shortly.

In the following we denote parameters in the diagonal lepton basis with a hat. Although we use  $\hat{\lambda}$  for illustration, the case of  $\hat{\lambda}'$  is similar. The dimensionless LNV couplings in the diagonal lepton basis,  $\hat{\lambda}_{abc}$  are related to the LNV couplings in the weak interaction basis,  $\lambda_{ijk}$ , by

$$\hat{\lambda}_{abc} = \lambda_{ijk} (Z_{lL}^\dagger)_{ai} (Z_{lL}^\dagger)_{bj} (Z_{lR})_{kc}. \quad (2.23)$$

The tree level neutrino mass matrix then scales (neglecting the sneutrino vevs) as

$$\begin{aligned} (\hat{\mathcal{M}}_{\text{eff}}^\nu)_{ab} &\propto \hat{\Lambda}_a \hat{\Lambda}_b \propto \hat{\mu}_a \hat{\mu}_b \propto \hat{\lambda}_{acd} (\hat{Y}_E^*)_{cd} \hat{\lambda}_{bef} (\hat{Y}_E^*)_{ef} \\ &= \left[ \lambda_{ijk} (Y_E^*)_{jk} \lambda_{nlm} (Y_E^*)_{lm} \right] (Z_{lL}^\dagger)_{ai} (Z_{lL}^*)_{nb}, \end{aligned} \quad (2.24)$$

and so

$$(\hat{\mathcal{M}}_{\text{eff}}^\nu)_{ab} = (Z_{lL}^\dagger)_{ai} (\mathcal{M}_{\text{eff}}^\nu)_{in} (Z_{lL}^*)_{nb}, \quad (2.25)$$

where  $\mathcal{M}_{\text{eff}}^\nu$  is the effective neutrino mass matrix in the original lepton flavour basis. The factorization of the two charged lepton mixings represents the shift of  $Z_{lL}$  from the charged lepton sector to the neutrino sector when computing  $U_{\text{PMNS}}$  using eq. (2.15). At loop level, we approximate its contribution to the full mass matrix by the dominating effect from  $\hat{\Sigma}_D$

$$(\hat{\Sigma}_D^\nu)_{ab} \simeq - \sum_{c,f} \sum_{d,e} \left\{ \frac{(\hat{m}_l^*)_{cf}}{(4\pi)^2} \hat{\lambda}_{acd} \hat{\lambda}_{bef} B_0(0, \hat{m}_{l_{de}}^2, \hat{m}_{l_{cf}}^2) + (a \leftrightarrow b) \right\} \quad (2.26)$$

in self-evident notation, and where  $B_0$  is a Passarino-Veltman function [44]. Using a mass

insertion approximation (MIA), one obtains

$$\begin{aligned}
 (\hat{\Sigma}_D^\nu)_{ab} &\simeq \sum_{c,f} \sum_{d,e} \left\{ \frac{(\hat{m}_l^*)_{cf}}{(4\pi)^2} \frac{\hat{\lambda}_{acd} \hat{\lambda}_{bef} (\hat{\mathcal{M}}_{lLR}^{2*})_{ed}}{(\hat{\mathcal{M}}_{lLL}^2)_{ee} - (\hat{\mathcal{M}}_{lRR}^2)_{dd}} \ln \left( \frac{(\hat{\mathcal{M}}_{lLL}^2)_{ee}}{(\hat{\mathcal{M}}_{lRR}^2)_{dd}} \right) + (a \leftrightarrow b) \right\} \\
 &= \sum_{\substack{i,j,k \\ n,l,m}} \sum_{d,e} \left\{ \frac{(m_l^*)_{jm}}{(4\pi)^2} \lambda_{ijk} \lambda_{nlm} \left[ \frac{(Z_{lL}^*)_{te} (\hat{\mathcal{M}}_{lLR}^{2*})_{ed} (Z_{lR}^T)_{dk}}{(\hat{\mathcal{M}}_{lLL}^2)_{ee} - (\hat{\mathcal{M}}_{lRR}^2)_{dd}} \ln \left( \frac{(\hat{\mathcal{M}}_{lLL}^2)_{ee}}{(\hat{\mathcal{M}}_{lRR}^2)_{dd}} \right) \right] \right. \\
 &\quad \left. + (i \leftrightarrow n) \right\} (Z_{lL}^\dagger)_{ai} (Z_{lL}^*)_{nb} \\
 &= \sum_{\substack{i,j,k \\ n,l,m}} \left\{ \frac{1}{(4\pi)^2} \lambda_{ijk} \lambda_{nlm} \frac{(m_l^*)_{jm} (\overline{\mathcal{M}}_{lLR}^{2*})_{lk}}{\overline{\mathcal{M}}_{lLL}^2 - \overline{\mathcal{M}}_{lRR}^2} \ln \left( \frac{(\overline{\mathcal{M}}_{lLL}^2)}{(\overline{\mathcal{M}}_{lRR}^2)} \right) \left[ 1 + \mathcal{O} \left( \frac{\delta \mathcal{M}^2}{\overline{\mathcal{M}}^2} \right) \right] \right. \\
 &\quad \left. + (i \leftrightarrow n) \right\} (Z_{lL}^\dagger)_{ai} (Z_{lL}^*)_{nb}, \tag{2.27}
 \end{aligned}$$

where  $\overline{\mathcal{M}}_{lLL(RR)}^2$  is a mean squared mass of the left (right) handed sleptons, and  $\delta \mathcal{M}^2$  represents deviation from such mean values. Note the index contraction of the  $\lambda$  in eq. (2.27) is different from those in eq. (2.24). However  $\hat{\Sigma}_D^\nu$  is dominated by the one LNV coupling that is non-zero at  $M_X$ , as all dynamically generated couplings are small compared with it. We then have  $i = n$ ,  $j = l$  and  $k = m$  and consequently  $\hat{\Sigma}_D^\nu$  is proportional to the tree level effective mass matrix  $\hat{\mathcal{M}}_{\text{eff}}^\nu$ , i.e.

$$(\hat{\Sigma}_D^\nu)_{ab} \propto (\hat{\mathcal{M}}_{\text{eff}}^\nu)_{ab}, \tag{2.28}$$

up to higher order corrections. It is unwieldy to write down the higher order corrections to this expression, with terms from many sources (e.g. RGE, mixing matrices including the charginos-lepton mixings and corrections in MIA) entering the next lowest order perturbation. The key result here is that the index contractions in eq. (2.24) and eq. (2.27) are different, unless they are dominated by a single LNV parameter, in which case they become proportional to each other. The tree level mass matrix is bilinear in  $\Lambda_i$ , which is proportional to  $\mu_i$ . The dynamical generation of  $\mu_i$  can be obtained by integrating their RGEs, which contain terms with odd powers of  $\lambda_{ijk}$  and  $\lambda'_{ijk}$ . On the other hand, one obtains the loop corrections to the neutrino mass matrix by summing over contributions which contain even powers of the LNV couplings. The interference between various contributions at tree level and at loop level are in general different as a result.

The scale of the light neutrino mass can be estimated by noting that in the case of degenerate charged lepton masses, there is an ambiguity in the definition of the charged lepton mixing. The Yukawa matrix is simply a unit matrix, which implies that our earlier discussion on one LNV coupling in a diagonal charged lepton basis will apply in this situation, and so there is only one massive neutrino. In other words, the light neutrino mass  $m_\nu^{\text{light}}$  arises from the deviation of charged lepton universality. Its mass is therefore expected to be suppressed relative to the heavy neutrino mass  $m_\nu^{\text{heavy}}$  by (the square of)

the ratio of the charged lepton mass to the scalar mass scale that appears in the loop, as well as the tree-loop scale difference coming from the RG evolution, ie

$$\frac{m_\nu^{\text{light}}}{m_\nu^{\text{heavy}}} \sim \mathcal{O}\left(\left(\frac{m_l}{m_{\tilde{l}}}\right)^2 \frac{1}{f^2}\right), \quad (2.29)$$

with  $f = f\left(\frac{\mu^2}{m_0^2}; \frac{A_0^2}{m_0^2}; \frac{\tilde{B}}{m_0^2}; \tan\beta\right)$  the function from eq. (2.20).

With more than one dominant LNV coupling, the situation is very different. By choosing appropriate LNV parameters, one can obtain a partial cancellation between the dimensionless LNV contributions in the dynamical generation of  $\mu_i$ , and suppress the tree level neutrino mass as a result. Also the above derivation of alignment relies on one coupling dominance, specifically  $i = n$ ,  $j = l$  and  $k = m$  eq. (2.27). Once we have more than one dominant coupling, this manipulation ceases to hold. As the alignment effect is weakened and the mass hierarchy becomes smaller, larger PMNS mixing is expected with large charged lepton mixing angles. So in the next minimal case with 2 LNV couplings at  $M_X$ , by allowing partial cancellations in the  $\mu_i$  generation and large charged lepton mixings, we may already be able to obtain the observed neutrino mass pattern. We will investigate this possibility by a numerical approach, discussed in the next section.

### 3. Numerical procedure

The parameter set that defines our model is given by

$$\begin{aligned} m_0, M_{1/2}, A_0, \text{sgn}\mu, @ M_X, \\ \theta_{12}^l, \theta_{13}^l, \theta_{23}^l, \Lambda_1, \Lambda_2 @ M_X, \\ \tan\beta @ M_Z, \end{aligned} \quad (3.1)$$

where

$$\Lambda_1, \Lambda_2 \in \{\lambda_{ijk}, \lambda'_{ijk}\}, \quad (3.2)$$

and  $M_X$  is defined to be the scale at which the electroweak gauge couplings unify.  $m_0$ ,  $M_{1/2}$  and  $A_0$  are the universal scalar mass, gaugino mass and SUSY breaking trilinear scalar coupling (divided by the corresponding Yukawa coupling) at  $M_X$  respectively. The sign of  $\mu$  is defined by  $\text{sgn}\mu$ . The charged lepton rotations are characterized by  $\theta^l$ 's in the standard parameterization [38], and  $\tan\beta$  is the ratio of the higgs vacuum expectation values  $v_u/v_d$ .

In the quark sector, flavour mixing is assumed to reside in the down-quark sector at the weak scale. We have also assumed that the down-quark Yukawa matrix  $Y_D$  is symmetric at that scale. In the lepton sector, we work with non-diagonal charged lepton Yukawa matrices, and define any non-zero LNV parameters in that flavour basis. The mixing angles  $\theta^l$  are determined by fitting the PMNS matrix. For definiteness, we assume that the two charged lepton mixings  $Z_{lL}$  and  $Z_{lR}$  are the same, or equivalently, that the charged lepton Yukawa matrix  $Y_E$  is symmetric.

The set of Lagrangian parameters (RPC and LNV) at  $M_Z$  are obtained using a modified version of the `SOFTSUSY` code [45]. At  $M_X$ , a set of dimensionless LNV parameters defined

in eq. (3.1) is chosen. At  $M_Z$ ,  $\tan\beta$ , the ratio of higgs vevs is also specified. The high scale LNV parameters are rotated to a diagonal charged lepton basis specified by  $\theta^l$ .

The parameters are run to  $M_Z$  using the full set of 1-loop MSSM RGEs including all LNV contributions, which are then required to match with the low scale boundary conditions on the gauge and Yukawa couplings. Throughout the analysis, we use  $m_t = 172.7$  GeV [46] and  $M_Z = 91.1876$  GeV for the pole masses of the top quark and the  $Z^0$  boson respectively. The weak scale gauge couplings in the  $\overline{MS}$  scheme are set to be  $\alpha^{-1}(M_Z) = 127.918$  and  $\alpha_s(M_Z) = 0.1187$ . Light quark masses are also set to their central values in the  $\overline{MS}$  scheme:  $m_b(m_b) = 4.25$  GeV,  $m_c(m_c) = 1.2$  GeV,  $m_s(2\text{GeV}) = 0.1175$  GeV,  $m_d(2\text{GeV}) = 0.00675$  GeV and  $m_u(2\text{GeV}) = 0.003$  GeV [38]. For the calculation of the physical Higgs mass and electroweak symmetry breaking (EWSB) conditions, one loop corrections are included.

To calculate the neutrino masses, we run the parameter set to

$$M_S = \sqrt{m_{\tilde{l}_1}(M_S)m_{\tilde{l}_2}(M_S)}, \quad (3.3)$$

where the EWSB conditions are imposed and all sparticle and Higgs pole masses are calculated in **SOFTSUSY**. The neutrino masses are obtained from the full  $7 \times 7$  neutrino-neutralino mass matrix including all LNV contributions at the 1-loop level. Throughout the calculation, the (s)lepton doublets are put on the same footing as  $H_d$ . Our analytic results were checked against ref. [25] for the full LNV case, and against ref. [41] in the RPC limit. Our numerical results agree well with ref. [25]. In the RPC limit, the neutralino corrections are also in agreement with the latest published version of **SOFTSUSY**.

After the initial rotation to a diagonal  $Y_E$  at  $M_X$ , the charged lepton matrix remains essentially diagonal at all renormalization scales due to the smallness of the LNV couplings. The computation of the PMNS mixings thus neglects all ‘residual’ flavour mixing generated through renormalization in the charged lepton sector. The three charged lepton mixing angles, together with the two GUT-scale LNV parameters are varied in order to obtain the best fit.

The minimization to find the best fit parameter set is performed using **MINUIT** [47] and the observables assumed in eq. (2.1).  $\chi^2$  is defined to be

$$\chi^2 = \sum_{i=1}^{N_{\text{obs}}} \left( \frac{f_i - O_i}{\sigma_i} \right)^2, \quad (3.4)$$

where  $O_i$  are the central values of the  $N_{\text{obs}}$  experimental observables,  $f_i$  are the corresponding numerical predictions, and  $\sigma_i$  are the 1-sigma uncertainties. We find that it is difficult to obtain convergence of a procedure which minimizes  $\chi^2$  when solar and atmospheric mass squared differences are included in  $O_i$  directly. We find a multi-step minimisation approach to be effective. In this approach, we first minimize a  $\chi^2$  of the mass ratio of the 2 heavy neutrinos and the sine squared of the three PMNS mixing angles by keeping one LNV parameter fixed. For a normal hierarchy we have

$$\begin{aligned} m_{\nu_1} &\sim 0, & m_{\nu_2} &= 8.9_{-0.16}^{+0.15} \times 10^{-3} \text{eV}, & m_{\nu_3} &= 5.10 \pm 0.20 \times 10^{-2} \text{eV}, & (3.5) \\ \Rightarrow \frac{m_3}{m_2} &= 5.74 \pm 0.32, \end{aligned}$$

whereas for an inverted hierarchy, we have

$$\begin{aligned}
 m_{\nu_1} &= 5.10 \pm 0.20 \times 10^{-2} \text{eV}, & m_{\nu_2} &= 5.18 \pm 0.19 \times 10^{-2} \text{eV}, & m_{\nu_3} &\sim 0, & (3.6) \\
 \Rightarrow \frac{m_2}{m_1} &= 1.0151 \pm 0.0769.
 \end{aligned}$$

At this stage, we obtain a good fit to the charged lepton mixing angles and the mass ratio but the values of the neutrino masses in general do not fit the atmospheric and solar mass squared differences. To perform a ‘proper’ fit we then switch to a  $\chi^2$  of  $\Delta m_{21}^2$ ,  $|\Delta m_{31}^2|$  as well as the three PMNS angles. We first fix the three charged lepton mixing angles and allow the two LNV parameters to vary. The LNV parameters will then adjust their values to fit the mass squared differences. Finally a full five parameter fit is performed. It is also helpful to have a good initial estimate of the size of the LNV parameter that is fixed in the first stage of minimization. We find that a suitable starting point is the value of the LNV coupling that saturates the one LNV coupling bound in [28], derived from the cosmological bound  $\sum_i m_{\nu_i} < 0.7 \text{eV}$  at 95% confidence level (CL) [48].

The above fitting is performed at  $M_S$ . After this, the resulting set of parameters is renormalized down to  $M_Z$ , where specific products of couplings are checked against the bounds in [27]. We also checked against the experimental bounds on the branching ratios of the processes  $l \rightarrow l'\gamma$  [49–51],  $B_s \rightarrow \mu^+\mu^-$  [52] and  $b \rightarrow s\gamma$  [53]. The bounds we use are

$$\begin{aligned}
 BR_{\text{exp}}(\mu \rightarrow e\gamma) &< 1.2 \times 10^{-11} && 90\% \text{CL}, \\
 BR_{\text{exp}}(\tau \rightarrow e\gamma) &< 1.1 \times 10^{-7} && 90\% \text{CL}, \\
 BR_{\text{exp}}(\tau \rightarrow \mu\gamma) &< 6.8 \times 10^{-8} && 90\% \text{CL}, && (3.7) \\
 BR_{\text{exp}}(B_s \rightarrow \mu^+\mu^-) &< 1.0 \times 10^{-7} && 95\% \text{CL}, \\
 2.76 \times 10^{-4} < BR(b \rightarrow s\gamma) &< 4.34 \times 10^{-4} && 2\sigma,
 \end{aligned}$$

where  $BR(b \rightarrow s\gamma)$  combines statistical and systematic experimental errors [54] together with a Standard Model theoretical error [55] by adding them in quadrature.

We have included a detailed calculation of  $BR(l \rightarrow l'\gamma)$  in appendix D. For a discussion of contributions of different couplings to this process, see e.g. [56]. The LNV contribution to  $BR(B_s \rightarrow \mu^+\mu^-)$  was calculated in [57]. A generalisation to include left-right mixings of the mediating squarks and non-degenerate sparticle masses can be found in [53]. The LNV contribution to  $BR(b \rightarrow s\gamma)$  in a leading log approximation is presented in [58].

One technical aspect that should be mentioned concerning the numerical calculation is the cancellation between the CP even (CPE) and the CP odd (CPO) scalar contributions to the neutrino masses at loop level. In the R-parity conserving limit, the CPE and CPO sneutrino contributions cancel exactly. When R-parity is violated, the higgses mix with the sneutrinos through the sneutrino vevs and the bilinear soft terms  $\tilde{D}_i$ , lifting the degeneracy of the masses of the CPE and CPO scalars. The mixing matrices of the CPE and CPO scalars also differ. This degeneracy lifting is in general very small compared with the sneutrino mass scale, but may have a significant impact on the neutrino masses.

Such a large cancellation is numerically unstable. In the phenomenologically interesting LNV parameter space, numerical fluctuations caused by such an instability are actually insignificant for weak scale sneutrinos. However away from this ‘good’ LNV region, the



second-lightest neutrino mass is usually highly suppressed compared to the third lightest (or the heaviest) neutrino as discussed in the previous section. Its eigenvalue can be dominated by numerical fluctuations, and tends to spoil the minimization procedure when the LNV parameter space away from the physically interesting region is accessed.

To get around this problem, we perform an analytic approximation commonly known as mass insertion approximation (MIA). We apply this technique to calculate the deviation from exact cancellation in the RPC limit, instead of performing the large numerical cancellation directly. In this calculation, it is useful to think of the  $5 \times 5$  neutral scalar matrices as a  $2 \times 2$  higgs block, a  $3 \times 3$  sneutrino block, and a  $2 \times 3$  block that mixes the higgses and the sneutrinos in the basis  $(h_u, h_d, \tilde{\nu}_e, \tilde{\nu}_\mu, \tilde{\nu}_\tau)$  as follows

$$\left(\mathcal{M}_{CPE(CPO)}^2\right)_{5 \times 5} = \begin{pmatrix} (M_{H(A)}^2)_{2 \times 2} & (\sigma_{H(A)})_{2 \times 3} \\ (\sigma_{H(A)}^T)_{3 \times 2} & (M_{\tilde{\nu}}^2)_{3 \times 3} \end{pmatrix}. \quad (3.8)$$

We take advantage of the fact that in the 't Hooft-Feynman gauge, the CPE and CPO sneutrino blocks  $M_{\tilde{\nu}}^2$  are identical and can be diagonalised by the same orthogonal matrix. The difference between the CPE and CPO contributions then come from  $M_{H(A)}^2$  and  $\sigma_{H(A)}$ . The CPE and CPO  $M^2$ 's can be separately diagonalised, leaving the off-diagonal contributions entirely in the (s)lepton number violating sector. In this basis it is possible to obtain successive corrections to the mixing matrices as well as the mass eigenvalues, or in our case their *difference* in terms of the small LNV parameters. We refer interested readers to [59] for a review of MIA. For details of our specific calculation, see appendix C.

#### 4. Results

For concreteness, we confine ourselves to the SPS1a [43] point with non-zero LNV couplings, i.e.

$$\begin{aligned} M_{1/2} &= 250\text{GeV}, & m_0 &= 100\text{GeV}, & A_0 &= -100\text{GeV}, \\ \text{sgn}\mu &= +1, & \tan\beta &= 10, \end{aligned} \quad (4.1)$$

although the numerical procedure can be applied equally well in other mSUGRA region. We first display an example with a normal hierarchy with non-zero  $\lambda_{233}$  and  $\lambda'_{233}$  at the unification scale. The set of best fit parameters is given by  $\theta_{12}^l = 0.460$ ,  $\theta_{13}^l = 0.389$ ,  $\theta_{23}^l = 0.305$ ,  $\lambda_{233} = 4.07 \times 10^{-5}$  and  $\lambda'_{233} = -2.50 \times 10^{-6}$ . The variation of the observables characterising the neutrino mass pattern with  $\lambda'_{233}$  is displayed in figure 3. We see in figure 3(a) that as  $\lambda'_{233}$  increases, the mass difference between the two heavy neutrinos decreases due to suppression of the tree level mass matrix and a weakening of the alignment effect. Eventually the mass difference increases again, signalling a cross over where the heaviest neutrino becomes dominated by contributions derived from  $\lambda'_{233}$ . In between there is a window which allows the mass squared differences to fall within the experimentally observed range, as displayed in figure 3(b). The variations of  $\sin^2\theta_{12}$  and  $\sin^2\theta_{13}$  shown in figure 3(c) and figure 3(d) are associated with the cross over described above, when the two mass eigenvectors determined by the two LNV parameters switch.

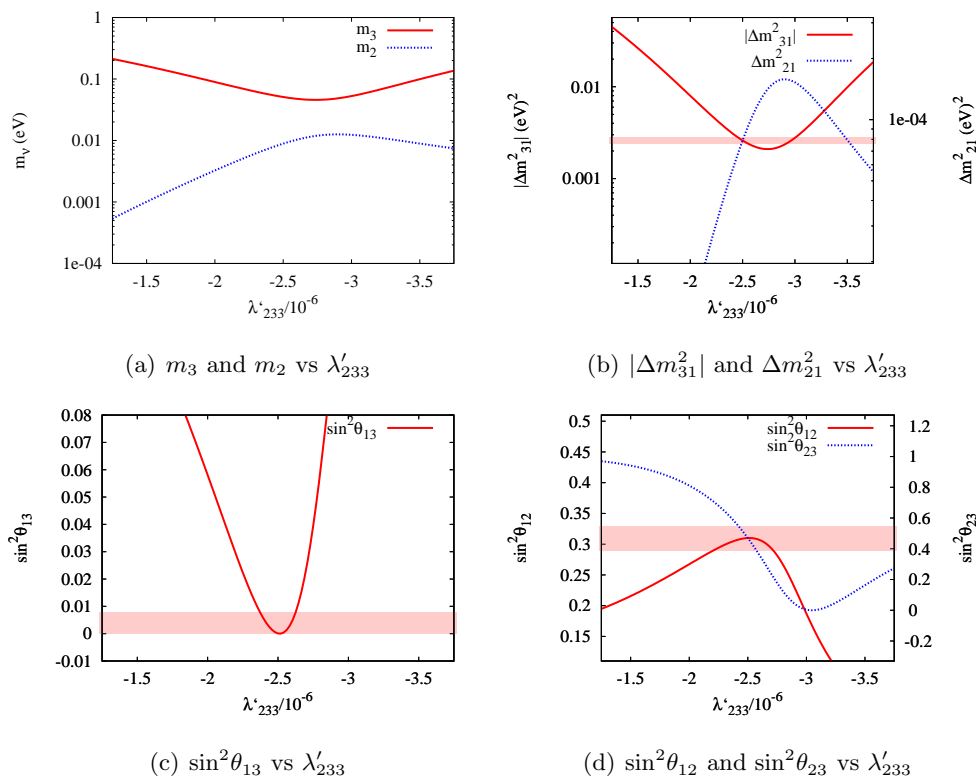


**Figure 3:** Variation of the observables characterising the neutrino mass pattern with  $\lambda_{233}$  at SPS1a in a normal hierarchy. The best fit parameters are  $\theta_{12}^l = 0.460$ ,  $\theta_{13}^l = 0.389$ ,  $\theta_{23}^l = 0.305$ ,  $\lambda_{233} = 4.07 \times 10^{-5}$  and  $\lambda'_{233} = -2.50 \times 10^{-6}$ . The strips display the empirical  $1\sigma$  bands.

In figure 4 we show an example with an inverted hierarchy, again with non-zero GUT-scale  $\lambda_{233}$  and  $\lambda'_{233}$ . The mass squared differences is much more sensitive to the variation of  $\lambda'_{233}$ , because of the larger cancellations required to obtain two near degenerate massive neutrinos. This reflects that fine tuning between the a priori unrelated  $\lambda_{233}$  and  $\lambda'_{233}$  couplings is required to generate the two quasi-degenerate mass scales in the inverted hierarchy. On the other hand, we see in figure 4(c) and figure 4(d) that  $\sin^2\theta_{13}$  and  $\sin^2\theta_{23}$  are insensitive to changes in  $\lambda'_{233}$ . This is because the lightest neutrino is almost massless, hence its flavour composition depends only weakly on variations in  $\lambda'_{233}$  once the mass degeneracy of the two initially light neutrinos are resolved by the presence of  $\lambda'_{233}$ . With an inverted hierarchy, this implies that the third column of  $Z_\nu$  is insensitive to the changes in the LNV couplings, which in the standard parameterization is determined fully by  $\theta_{13}$  and  $\theta_{23}$ .<sup>7</sup> Of course,  $\sin^2\theta_{12}$  will still change as shown in figure 4(d), which again is associated with the cross-over of the two heavy mass eigenstates.

For an inverted hierarchy, in principle there may be sizeable two loop corrections which could affect the delicate balance among terms in the effective neutrino mass matrix. However, the two loop corrections in question are not in the literature. We expect the main

<sup>7</sup>There is also a dependence on the Dirac CP violating phase  $\delta$ , but it is suppressed by the smallness of  $\sin^2\theta_{13}$ , and we assume CP conservation throughout our numerical analysis.

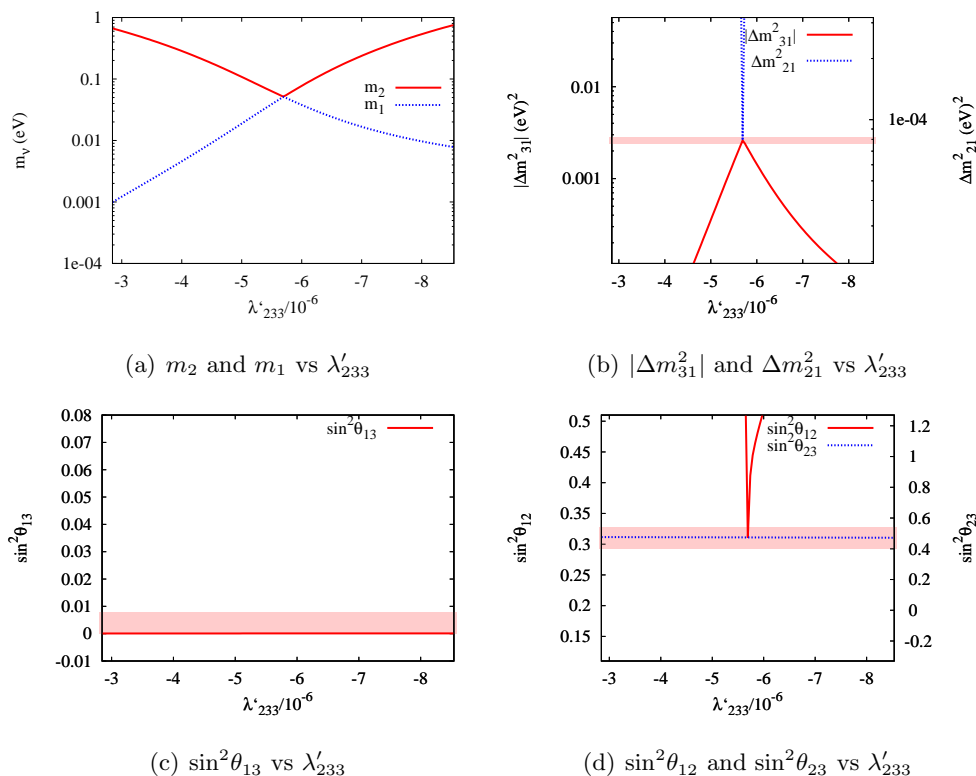


**Figure 4:** Variation of the observables characterising the neutrino mass pattern with  $\lambda'_{233}$  at SPS1a with an inverted hierarchy. The best fit parameters are  $\theta_{12}^l = 1.55779$ ,  $\theta_{13}^l = 0.815115$ ,  $\theta_{23}^l = 0.146126$ ,  $\lambda_{233} = 1.36023 \times 10^{-4}$  and  $\lambda'_{233} = -5.69116 \times 10^{-6}$ . The strips display the empirical  $1\sigma$  bands. The lines  $\theta_{13}$  and  $\theta_{23}$  are essentially flat.

corrections to come from the strong interaction, and possibly from heavy flavours. Smaller corrections may be found, for example, in [60]. We attempted to estimate these 2-loop effects by scaling the 1-loop quark contributions. For the parameter sets displayed in tables 1 and 2, it was shown that an universal 10% variation leads to a change in  $\chi^2$  of the order 30 for an inverted hierarchy. However, after re-fitting all  $\chi^2$ 's go back to the level before scaling, and the change in the best fit parameters is negligible. For a normal hierarchy, the change in  $\chi^2$  is of the order 0.01, and the changes in re-fitted parameters as well as  $\chi^2$  are again negligibly small. Therefore, although more careful analysis of the two loop effects is probably required, we do not expect the possibility of finding modified best fit solutions with two nearly degenerate mass eigenstates in an inverted hierarchy to be affected.

We have described in the previous sections that the tree level mass needs to be suppressed relative to a ‘natural’ value of order given by eq. (2.16). As shown in figure 3 and figure 4, this can be achieved by a partial cancellation between the two LNV couplings. To quantify the amount of tuning required, we follow ref. [61] and define a fine tuning measure  $\Delta_{\text{FT}}$  by

$$\Delta_{\text{FT}} = \left| \frac{\partial \ln(\mathcal{O}(\lambda'))}{\partial \ln \lambda'} \right|, \tag{4.2}$$

where  $\mathcal{O}$  is either  $\Delta m_{21}^2$  or  $|\Delta m_{31}^2|$ , whichever gives a larger  $\Delta_{\text{FT}}$ . It can be seen in figure 3(b) that for a normal hierarchy, the two observables result in similar  $\Delta_{\text{FT}}$ . However for the inverted hierarchy,  $\Delta_{\text{FT}}$  is determined by  $\Delta m_{21}^2$ , see figure 4(b). The second case can be understood from the fact that  $\Delta m_{21}^2$  arises from the *difference* between  $m_1$  and  $m_2$ , both of which are of order  $\mathcal{O}(\sqrt{|\Delta m_{31}^2|})$ . The variation of  $\Delta m_{21}^2$  is then expected to be of order  $\mathcal{O}(|\Delta m_{31}^2|)$ , the latter of which is significantly larger than the solar mass difference. We obtain numerical values for the fine tuning measure by

$$\Delta_{\text{FT}} \simeq \left| \frac{\ln(\mathcal{O}(\lambda'_a)) - \ln(\mathcal{O}(\lambda'_b))}{\ln \lambda'_a - \ln \lambda'_b} \right|, \tag{4.3}$$

where  $\lambda'_b$  is the best fit value, and  $\lambda'_a$  is given by

$$\lambda'_a = \lambda'_b \times (1 - 2.0 \times 10^{-4}). \tag{4.4}$$

For the normal hierarchy,  $\Delta_{\text{FT}}$  works out to be of order  $\mathcal{O}(10)$ , so the level of fine tuning is mild compared with other SUSY parameters (see e.g. ref. [62]). However for the inverted hierarchy,  $\Delta_{\text{FT}}$  is typically of order  $\mathcal{O}(700 - 1000)$ . In this sense, the present study shows a preference towards a normal hierarchy.

In tables 1 and 2, we present a collection of parameter sets that minimizes the  $\chi^2$  defined in section 3. We also display the values of  $\Delta_{\text{FT}}$ . Naturally not all parameter combinations result in good fits of the observed parameters listed in eq. (2.1). Note however that we do not attempt to exhaust all possibilities within this 2 LNV parameters setting. Also, not all LNV parameter combinations result in satisfactory numerical convergence. While some is due to flavour structure incompatible with the requirement of tree level suppression, others are due to problems encountered in the minimization, for example running into a corner in the parameter space. Bearing this in mind, a few comments can be made:

- Because the LNV couplings involved are all very small, the sparticle mass spectrum remains essentially the same as in SPS1a, and all branching ratios of the sparticles are unaffected except for that of the LSP.
- It is not possible to obtain the observed mass hierarchy with 2  $\lambda'$ 's, because in order to suppress the tree-loop mass scale difference, the two  $\lambda'$ 's need to violate the same lepton flavour in order to contribute to the same  $\mu_i$  for the cancellation to occur. However, with only one flavour violated, there can only be one massive neutrino.
- The successful parameter sets that fit the data all consist of one  $\lambda$  and one  $\lambda'$  coupling. In principle it is possible to have two  $\lambda$ 's, which might be more interesting because this implies the LSP will decay almost exclusively via leptonic channels. Indeed if the assumption of  $Z_{lL} = Z_{lR}$  is relaxed, we find parameter sets with two dominant  $\lambda$  couplings.
- Typically all three charged lepton mixing angles are large. This means that we expect many competing decay channels for the LSP, even though we only have 2 non-zero LNV couplings in the weak interaction basis. As an example, we display in tables 3

and 4 the major LSP decay channels with  $\lambda_{233}$  and  $\lambda'_{233}$ , for a normal hierarchy and for an inverted hierarchy respectively.

- Although we focus on the SPS1a point, in which the LSP is a neutralino, it is also interesting to consider scenarios with e.g. stau LSP. In the latter case, a back of an envelope calculation shows that for a 4 body decay to dominate, one typically requires (in the diagonal charged lepton basis) LNV couplings with no stau index to be roughly 4 orders of magnitude larger than the couplings with a stau index. This seems unlikely given the necessarily large charged lepton mixings.
- The lightest neutrino mass is negligible in the current set up. Given this, the other two neutrino masses can be obtained using the atmospheric and solar mass squared values. Regardless of whether one assumes the inverted or natural hierarchy, the resulting neutrino mass sum automatically satisfies the cosmological bound  $\sum_i m_{\nu_i} < 0.7 \text{ eV}$ . However, the size of the couplings at  $M_Z$  can still be comparable to the single coupling bounds obtained in [28] based on the cosmological bound. This is because the required cancellation for the tree level mass suppression makes the couplings larger than what would be naively expected.
- Roughly speaking, for sparticle mass of  $\mathcal{O}(100) \text{ GeV}$ , the LNV coupling products involving  $\lambda\lambda$  or  $\lambda'\lambda'$  need to be of order  $\sim \mathcal{O}(10^{-6})$  to have any chance to saturate the  $BR(\mu \rightarrow e\gamma)$  bound, and are less stringent for the other two leptonic FCNC. These can be estimated readily using the analytical expressions in appendix D. For  $BR(B_s \rightarrow \mu^+\mu^-)$ , the coupling products need to be at least of  $\mathcal{O}(10^{-5})$  [57], whereas for  $BR(b \rightarrow s\gamma)$  the coupling products need to be of  $\mathcal{O}(10^{-2})$  [58]. Clearly the couplings involved in our cases are too small to contribute significantly to these rare decays, but we have also checked numerically that this is indeed the case.
- If the LSP is a stau, it is expected to decay promptly at the interaction point. If the LSP is a neutralino, it decays into 3 SM fermions. Assuming a pure photino LSP, an order of magnitude estimate for the 3 body decay is given by [63]

$$\Gamma(\tilde{\chi}_1^0 \rightarrow fff) = \frac{n_c \alpha (\lambda \text{ or } \lambda')^2}{128\pi^2} \frac{m_{\tilde{\chi}_1^0}^5}{M_{\text{SUSY}}^4}, \quad (4.5)$$

where the  $f$ 's denote SM fermions,  $n_c$  is the number of colours,  $\alpha$  is the fine structure constant, and  $M_{\text{SUSY}}$  is the mass scale of the virtual, intermediate scalar. For the results displayed in tables 1 and 2, the neutralino can decay with a displaced vertex of  $\mathcal{O}(0.1)\text{mm}$  (the total width is of order  $\mathcal{O}(10^{-12} - 10^{-11})\text{GeV}$ ). Such a displacement would not be immediately obvious, but could be searched for, providing additional confirmation.

- For the inverted hierarchy, due to the high degree of tuning, all digits presented in table 2 are needed in order to produce the correct neutrino oscillation parameters.

$\Lambda_1$	$\Lambda_2$	$\theta_{12}^l$	$\theta_{13}^l$	$\theta_{23}^l$	$\Delta_{\text{FT}}$
$^a \lambda'_{233} = -2.49978 \times 10^{-6}$	$\lambda_{233} = 4.06508 \times 10^{-5}$	0.459520	0.388989	0.304863	8.09
$^a \lambda'_{233} = -2.50019 \times 10^{-6}$	$\lambda_{211} = 4.06533 \times 10^{-5}$	1.98935	1.08162	0.632130	8.10
$^a \lambda'_{233} = -3.41336 \times 10^{-6}$	$\lambda_{321} = 9.86746 \times 10^{-5}$	0.448321	0.400030	2.89062	12.4
$^b \lambda'_{122} = -1.14066 \times 10^{-4}$	$\lambda_{122} = 4.06346 \times 10^{-5}$	1.19298	0.190538	1.17391	11.8
$^b \lambda'_{122} = -8.97777 \times 10^{-5}$	$\lambda_{123} = 1.02771 \times 10^{-4}$	2.10672	0.174800	1.18124	9.44
$^b \lambda'_{122} = -8.59626 \times 10^{-5}$	$\lambda_{133} = 4.09647 \times 10^{-5}$	0.997963	0.281922	0.417935	8.00
$^\dagger \lambda'_{311} = -8.34433 \times 10^{-4}$	$\lambda_{311} = 4.09870 \times 10^{-5}$	2.01028	1.07090	2.18984	8.00
$^\dagger \lambda'_{311} = -1.14183 \times 10^{-3}$	$\lambda_{321} = 9.88004 \times 10^{-5}$	0.448302	0.400044	1.32004	12.4
$^\dagger \lambda'_{311} = -8.66312 \times 10^{-4}$	$\lambda_{132} = 9.85792 \times 10^{-5}$	0.921694	-1.12754	2.00207	9.26
$^\dagger \lambda'_{233} = -4.07409 \times 10^{-5}$	$\lambda'_{211} = 8.36075 \times 10^{-4}$	0.457859	0.390978	0.304896	8.08
$^\dagger \lambda'_{233} = -4.07226 \times 10^{-5}$	$\lambda'_{221} = 4.16596 \times 10^{-4}$	0.458736	0.389932	0.304588	8.09
$^\dagger \lambda'_{233} = -4.06542 \times 10^{-5}$	$\lambda'_{231} = 7.40962 \times 10^{-4}$	0.459528	0.388981	0.304805	8.09

**Table 1:** A selection of LNV parameters and charged lepton mixings at SPS1a which fit the neutrino masses and mixings for a normal hierarchy. All the points shown have  $\chi^2 < 10^{-3}$ . The parameter sets marked with  $\dagger$  are ruled out by the  $\mu\text{Ti} \rightarrow e\text{Ti}$  constraints in [27].

$\Lambda_1$	$\Lambda_2$	$\theta_{12}^l$	$\theta_{13}^l$	$\theta_{23}^l$	$\Delta_{\text{FT}}$	$\chi^2$
$^a \lambda'_{233} = -5.69116 \times 10^{-6}$	$\lambda_{233} = 1.36023 \times 10^{-4}$	1.55779	0.815115	0.146126	755	0.01
$^a \lambda'_{233} = -5.69126 \times 10^{-6}$	$\lambda_{211} = 1.32365 \times 10^{-4}$	1.38843	0.760045	0.140903	758	0.06
$^a \lambda'_{233} = -5.67940 \times 10^{-6}$	$\lambda_{123} = 1.42938 \times 10^{-4}$	1.81386	-0.757538	0.141975	726	0.05
$^b \lambda'_{122} = -1.96283 \times 10^{-4}$	$\lambda_{122} = 1.24824 \times 10^{-4}$	0.134765	0.101938	0.798282	988	0.43
$^b \lambda'_{122} = -1.93673 \times 10^{-4}$	$\lambda_{132} = 1.47364 \times 10^{-4}$	3.03234	0.0866645	0.931616	743	2.85
$^b \lambda'_{122} = -1.96175 \times 10^{-4}$	$\lambda_{123} = 1.45708 \times 10^{-4}$	0.144386	0.0943266	0.689708	736	0.52
$^\dagger \lambda'_{311} = -1.90386 \times 10^{-3}$	$\lambda_{311} = 1.16446 \times 10^{-4}$	1.76438	0.833990	1.40752	767	1.41
$^\dagger \lambda'_{311} = -1.90027 \times 10^{-3}$	$\lambda_{321} = 1.44392 \times 10^{-4}$	1.52379	0.854066	1.42182	719	0.22
$^\dagger \lambda'_{311} = -1.90809 \times 10^{-3}$	$\lambda_{322} = 1.37574 \times 10^{-4}$	1.57829	0.820421	1.42557	984	0.01
$^\dagger \lambda'_{233} = -1.36245 \times 10^{-4}$	$\lambda'_{211} = 1.90793 \times 10^{-3}$	1.55054	0.815304	0.146304	979	0.01
$^\dagger \lambda'_{233} = -1.36235 \times 10^{-4}$	$\lambda'_{221} = 9.50337 \times 10^{-4}$	1.55302	0.815293	0.146092	975	0.00
$^\dagger \lambda'_{233} = -1.36016 \times 10^{-4}$	$\lambda'_{231} = 1.68685 \times 10^{-3}$	1.56378	0.815077	0.145634	753	0.00

**Table 2:** A selection of LNV parameters and charged lepton mixings at SPS1a which fit the neutrino masses and mixings for an inverted hierarchy. The parameter sets marked with  $\dagger$  are ruled out by the  $\mu\text{Ti} \rightarrow e\text{Ti}$  constraints in [27]. Note that because of the high fine tuning, all digits present in the table are required to obtain the correct numerical results.

As mentioned in section 3, the numerical analysis is performed in a basis where all quark mixings reside in the down quark sector. In the case of up type quark mixings, only  $\lambda'$  couplings with the same quark flavour indices can be used to balance the contribution of  $\lambda$  in the dynamical generation of the bilinear parameters, because the down quark Yukawa matrix  $Y_D$  is diagonal in this basis. Apart from this, the main effect in changing the quark mixing is expected to be a rescaling of  $\lambda'$ , with only minor changes to  $\lambda$  and the charged lepton mixing angles. This is confirmed by our numerical results.

In tables 3 and 4, the branching ratios of the neutralino LSP for non-zero  $\lambda_{233}$  and  $\lambda'_{233}$  with the normal and inverted hierarchy respectively are generated using ISAJET7.64 [64].

$\lambda_{ijk}$	Channel	BR	Channel	BR
$\lambda_{122}$	$e^- \nu_\mu \mu^+$	0.006	$\mu^- \nu_e \mu^+$	0.006
$\lambda_{132}$	$e^- \nu_\tau \mu^+$	0.007	$\tau^- \nu_e \mu^+$	0.007
$\lambda_{123}$	$e^- \nu_\mu \tau^+$	0.029	$\mu^- \nu_e \tau^+$	0.029
$\lambda_{133}$	$e^- \nu_\tau \tau^+$	0.034	$\tau^- \nu_e \tau^+$	0.034
$\lambda_{231}$	$\mu^- \nu_\tau e^+$	0.005	$\tau^- \nu_\mu e^+$	0.005
$\lambda_{232}$	$\mu^- \nu_\tau \mu^+$	0.027	$\tau^- \nu_\mu \mu^+$	0.028
$\lambda_{233}$	$\mu^- \nu_\tau \tau^+$	0.138	$\tau^- \nu_\mu \tau^+$	0.140

**Table 3:** Decay channels of the LSP  $\tilde{\chi}_1^0$  at SPS1a, with  $\lambda_{233}$  and  $\lambda'_{233}$  at  $M_X$  given in the top row of table 1, and a normal hierarchy. Each process has a charged conjugated counterpart which is not shown in the table. Only branching ratios  $\geq 0.005$  are displayed.

$\lambda_{ijk}$	Channel	BR	Channel	BR
$\lambda_{122}$	$e^- \nu_\mu \mu^+$	0.063	$\mu^- \nu_e \mu^+$	0.063
$\lambda_{132}$	$e^- \nu_\tau \mu^+$	0.056	$\tau^- \nu_e \mu^+$	0.057
$\lambda_{123}$	$e^- \nu_\mu \tau^+$	0.067	$\mu^- \nu_e \tau^+$	0.067
$\lambda_{133}$	$e^- \nu_\tau \tau^+$	0.059	$\tau^- \nu_e \tau^+$	0.060

**Table 4:** Decay channels of the LSP  $\tilde{\chi}_1^0$  at SPS1a, with  $\lambda_{233}$  and  $\lambda'_{233}$  at  $M_X$  shown in the top row of table 2, and an inverted hierarchy. Each process has a charge-conjugated counterpart which is not shown in the table. Only branching ratios  $\geq 0.005$  are displayed.

In both cases there are many competing channels for the LSP decay, not surprising due to the typically large charged lepton mixing. On the other hand, it is amusing to observe the approximate left handed  $\mu - \tau$  symmetry for the normal hierarchy, and approximate  $\mu - \tau$  symmetry for *both* chiralities in the inverted hierarchy. This corresponds to an approximate symmetry among the  $\lambda$  couplings after rotating to the diagonal charged lepton basis, and should be compared with the approximate  $\mu - \tau$  symmetry in the experimentally favored near tri-bi maximal neutrino mass matrix [65]. This effect appears in all parameter sets we have checked which give rise to the observed neutrino mass pattern. However the result depends on the assumed condition of  $Z_{lL} = Z_{lR}$ . We have checked that in other basis, for example with  $Z_{lR} = 1_{3 \times 3}$ , this approximate symmetry ceases to appear.

Another observation is that the dominant decay channels in these two samples are purely leptonic despite the presence of the  $\lambda'$  couplings. This is mainly due to the choice of the third family indices in  $\lambda'_{233}$ , which involves bottom Yukawa couplings in the dynamical generation of  $\mu_i$ . The cancellation condition then requires this coupling to be relatively small. In cases with  $\lambda'$  coupling which involves smaller quark Yukawa couplings, the 3 body decay via this coupling can become dominant. Then, LSP decays into a charged lepton plus jets and some SUSY production events may be fully reconstructed since there would be no intrinsic missing energy.

## 5. Discussion

We have shown that it is possible to obtain the observed neutrino mass pattern with 2 trilinear lepton number violating parameters in the mSUGRA set up in a basis where the lepton Yukawa coupling matrix is non-diagonal. However, depending on the flavour structure, the two non-zero couplings can either have one dominate over another, or have comparable magnitude. Here, we do not address the origin of hierarchies in the GUT-scale dimensionless couplings. They may be set, for example, by a spontaneously broken U(1) family gauge symmetry [66]. As an illustration, the first three parameter sets shown, labelled with superscripts (a), in both tables 1 and 2 have  $\lambda'_{233}$  a factor  $\sim \mathcal{O}(10)$  smaller than the other LNV operator and so may be described by flavour models with only one dominant operator. For the next three parameter sets labelled with superscripts (b),  $\lambda_{1ij}$  and  $\lambda'_{122}$  are of similar magnitude. A rough indicator of whether particular LNV parameters may contribute significantly to the neutrino mass may be defined by noting that the dynamical generation of  $\mu_i$  scales like  $\lambda(Y_E^*) + 3\lambda'(Y_D^*)$  from eq. (2.17). As an example suppose we are able to identify one coupling, say  $\lambda_{ikl}$ , that contribute to the neutrino mass matrix significantly. Other couplings will also be important if

$$\frac{\lambda_{ikl}}{\lambda'_{jmn}} \simeq \frac{(Y_D^*)_{mn}}{(Y_E^*)_{kl}}, \quad (5.1)$$

where the Yukawa couplings are evaluated in the weak interaction basis. Whether we have single coupling dominance or not can then be estimated by the ratio of the Yukawa couplings. However, for an inverted hierarchy, a slight change in the neutrino mass matrix can modify the results significantly, so more care is needed when applying this rough indicator.

In the following we briefly compare our models with the literature. In neutrino models with bilinear R-parity violation, e.g. [17, 30, 18], the vacuum oscillation solution is generally favoured. This is due to the alignment effect which creates a large hierarchy between the tree level mass and the loop induced masses. Because we are interested in models with only trilinear R-parity violation at the unification scale, we make no further comments on this and refer interested readers to the literature.

In [23], models with many  $\lambda'_{ijk}$  couplings are discussed. It was shown how such models naturally lead to the now excluded vacuum oscillation solution of the solar neutrino problem. Our work complement such results by discussing the issues need to be addressed for a near tri-bi maximal mixing solution, and also performs the numerical calculation by considering the full set of RGEs and include all one-loop contributions to the neutrino masses.

In [33], fits on the neutrino masses in LNV mSUGRA using trilinear couplings in the diagonal lepton basis were attempted. The need for tree level mass suppression and the need to break the alignment effect were also discussed there. A hierarchy was assumed which included only the terms  $\lambda'_{i33}$  and/or  $\lambda_{i33}$  as a first approximation. This requires a different tree mass suppression method involving the RPC soft SUSY breaking parameters, whereas in our work, the suppression is obtained through interplay among the LNV parameters. The RGEs used in our work also included the contributions of the quarks and leptons from the first and second generations to the soft SUSY breaking terms. These can be important



as, depending on their size, the LNV couplings with first and second generation indices may contribute significantly to the neutrino masses through coupling to the RPC Yukawa matrices in the RG equations. This also allows us to go beyond the natural hierarchy assumed in [33]. Preference towards the small mixing angle MSW solution was preferred in their analysis, but only the mass squared differences and the atmospheric mixing angle was fitted. In our work, we obtain the best fit values of the LNV parameters with all 3 PMNS mixing angles as well as the mass squared differences.

In [25], the authors described how the tri-bi maximal mixing pattern may be obtained by setting particular combinations of LNV parameters at the electroweak scale, which essentially involves setting two set of parameters, each with a different scale, to fit the observed neutrino mass pattern with the two scales  $|\Delta m_{31}^2|$  and  $\Delta m_{21}^2$ . Besides working in different basis, our models are in general inequivalent, because by setting the LNV couplings at  $M_Z$ , the problem associated with a tree-loop hierarchy is absent, and the mass scales involved can be set directly, without any need of tree-loop level cancellation. Depending on the parameters chosen, it is even possible to have a vanishing tree level contribution in such models. The models presented in this paper are more difficult to control in this sense because the two mass scales involved are related by the (suppressed) dynamical generation of the bilinear terms. In a similar spirit, ref. [67] assumes ansatzes for the weak-scale tri-linear LNV couplings in terms of six parameters. Some resulting models were shown to fit low-energy bounds as well as the atmospheric and solar neutrino anomalies. Some implications for LHC signals were investigated.

Finally, we comment on the amount of tuning required. It may appear that the cancellation required is unnatural. To some extent we do need certain degree of tuning. We must cancel the tree-level mass sufficiently such that the loop corrections are roughly  $\mathcal{O}(0.1)$  times the tree level mass for a normal hierarchy. This implies that  $\mu_i$  is suppressed by  $\mathcal{O}(1)$  compared to its ‘natural’ scale. This intuition is in agreement with the fine tuning measure discussed in section 4. For an inverted hierarchy, the loop corrections need to be roughly of the same order of magnitude as the tree level piece, and the solar neutrino mass difference arises from the difference between the masses of the two heaviest neutrinos, both of which are of the atmospheric mass scale. This means that while the parameters do need to be fine tuned for an inverted hierarchy due to the small solar neutrino mass difference compared to the atmospheric mass difference, for the normal hierarchy the tuning is reasonably mild. Once the tree and the loop contributions to the neutrino masses become comparable, we see that the suppression of tree level mass also leads to departure from alignment, and significant neutrino mixing results if one allows for charged lepton mixings, possibly provided by some underlying flavour model. Thus large PMNS mixing is not unreasonable, although we have to treat the experimentally favoured near tri-bi maximal neutrino mass pattern as accidental in our approach.

To summarise, we have investigated the minimal configuration in mSUGRA with tri-linear R-parity violation that can reproduce the observed neutrino oscillation observables. We obtain this by adding lepton *number* violating parameters in a basis where the charged lepton Yukawa matrix is not diagonal. We discuss on general grounds that it is impossible to obtain the neutrino mass hierarchy with just one LNV parameter in such a basis. This

can be traced to the fact that the bilinear lepton number violating operators responsible for the tree level mass generation are radiatively generated by the trilinear coupling. Despite the radiative origin of the bilinear operators, it turns out the tree level mass scale is dominant over the loop mass scale. Another general result is the alignment effect, whereby the tree level mass matrix and the loop corrections have almost the same pattern, therefore suppressing the light neutrino mass further.

These effects can already be alleviated by introducing a second trilinear operator at  $M_X$ . The reason is that the bilinear operators will be suppressed if the trilinear operators contribute to their dynamical generations in an opposite way. The introduction of another dominant coupling also weakens the alignment, and the PMNS mixings observed can be obtained with large charged lepton mixings.

We present, for both hierarchies, several data sets at SPS1a obtained by minimizing the chi-square of the neutrino oscillation observables. The couplings involved are too small to affect the spectrum and decay of the sparticles, except for the LSP, which has to decay via the LNV operators. We find typically that there are a number of significant decay channels, while the actual channels are model dependent. Depending on the choice of the  $\lambda'$  coupling, certain parameter sets are ruled out by the  $\mu - e$  conversion in nuclei, but the LNV contributions to the branching ratios for other FCNCs considered are typically not experimentally accessible.

While we need a certain degree of tuning to ensure the mass ratios fall in the observed range, the degree of tuning required for a normal mass hierarchy is relatively mild with  $\Delta_{\text{FT}} \sim \mathcal{O}(10)$ . The fine tuning required for the inverted hierarchy  $\Delta_{\text{FT}} \sim \mathcal{O}(800)$  reflects the need to arrange two a priori unrelated parameters to give two (quasi-) degenerate masses to account for the small solar neutrino mass squared difference.

Evidently with so many lepton number violating operators, there are many ways to reconstruct the neutrino mass matrix. While we have shown that it is possible to build simple models with a manageable LNV parameter space, future work is required to realize the many other possibilities within this class of models.

## Acknowledgments

This work has been partially supported by STFC. We thank the members of the Cambridge SUSY working group and S Rimmer for useful conversations. The computational work has been performed using the Cambridge eScience CAMGRID computing facility, with the invaluable help of Mark Calleja. CHK is funded by a Hutchison Whampoa DHPA studentship.

## A. Mass matrices

In this section we write down the CP-even, CP-odd, neutral fermion and charged fermion mass matrices. The notation follows that in [28], where the mass matrices are presented in terms of couplings in the Lagrangian. However following SOFTSUSY, the Standard Model

Higgs vev is normalized to  $v \approx 246\text{GeV}$ . The ‘t Hooft Feynman gauge is used for numerical computation, although we present the mass matrices in the general  $\xi$  gauge.

Our convention is the same as in [25] where all mass matrices are presented in 2-component Weyl notation (apart from the inclusion of the sneutrino vevs). We also follow their definition of the mixing matrices. In the R-Parity conserving case, the mass matrices reduce to those in [41].<sup>8</sup>

With LNV, the down type higgs and the lepton doublets are put on the same footing. It is therefore instructive to write down the superpotential and the Lagrangian in a way that express this equivalence. We define

$$\mathcal{L}_\alpha \equiv (H_d, L_i), \tag{A.1}$$

where  $\alpha, \beta, \dots \in \{0, 1, 2, 3\}$  and  $i, j, k, \dots \in \{1, 2, 3\}$ . The parameters are defined by

$$\begin{aligned} \lambda_{\alpha\beta k} &\equiv \left( \lambda_{0jk} \equiv (Y_E)_{jk}, \lambda_{ijk} \right), & h_{\alpha\beta k} &\equiv \left( h_{0jk} \equiv (h_E)_{jk}, h_{ijk} \right), \\ \lambda'_{\alpha jk} &\equiv \left( \lambda'_{0jk} \equiv (Y_D)_{jk}, \lambda'_{ijk} \right), & h'_{\alpha jk} &\equiv \left( h'_{0jk} \equiv (h_D)_{jk}, h'_{ijk} \right), \\ \mu_\alpha &\equiv (\mu, \mu_i), & b_\alpha &\equiv (\tilde{B}, \tilde{D}_i), \end{aligned} \tag{A.2}$$

and

$$(m_{\mathcal{L}}^2)_{\alpha\beta} \equiv \left( (m_{\mathcal{L}}^2)_{00} \equiv m_{h_d}^2, (m_{\mathcal{L}}^2)_{0i} \equiv m_{h_d L_i}^2, (m_{\mathcal{L}}^2)_{ij} \equiv (m_{\tilde{L}}^2)_{ij} \right). \tag{A.3}$$

In this notation, the superpotential is written as

$$\mathcal{W} = \frac{1}{2} \lambda_{\alpha\beta k} \mathcal{L}_\alpha \mathcal{L}_\beta \bar{E}_k + \lambda'_{\alpha jk} \mathcal{L}_\alpha Q_j \bar{D}_k + (Y_U)_{ij} Q_i H_u \bar{U}_j - \mu_\alpha \mathcal{L}_\alpha H_u, \tag{A.4}$$

while the soft supersymmetry breaking Lagrangian is denoted to be

$$\begin{aligned} -\mathcal{L}_{\text{soft}} &= \frac{1}{2} h_{\alpha\beta k} \tilde{\mathcal{L}}_\alpha \tilde{\mathcal{L}}_\beta \tilde{\bar{E}}_k + h'_{\alpha jk} \tilde{\mathcal{L}}_\alpha \tilde{Q}_j \tilde{\bar{D}}_k - b_\alpha \tilde{\mathcal{L}}_\alpha h_u + (h_U)_{ij} \tilde{Q}_i h_u \tilde{\bar{U}}_j + h.c. \\ &+ \tilde{\mathcal{L}}^\dagger (m_{\tilde{\mathcal{L}}}^2) \tilde{\mathcal{L}} + \tilde{\bar{E}}^\dagger (m_{\tilde{E}}^2) \tilde{\bar{E}} + m_{h_u}^2 h_u^\dagger h_u + \tilde{Q}^\dagger (m_{\tilde{Q}}^2) \tilde{Q} + \tilde{\bar{U}}^\dagger (m_{\tilde{U}}^2) \tilde{\bar{U}} + \tilde{\bar{D}}^\dagger (m_{\tilde{D}}^2) \tilde{\bar{D}} \\ &+ \left[ \frac{1}{2} M_1 \tilde{B} \tilde{B} + \frac{1}{2} M_2 \tilde{W} \tilde{W} + \frac{1}{2} M_3 \tilde{g} \tilde{g} + h.c. \right]. \end{aligned} \tag{A.5}$$

The mass matrices presented below follow the above notation.

### Higgs-sneutrino masses

After electroweak symmetry breaking, the sneutrinos,  $\tilde{\nu}_i$  mixes with the Higgs bosons  $h_u$  and  $h_d \equiv \tilde{\nu}_0$ , resulting in CP-even (CPE) and CP-odd (CPO) scalars. The CPE and CPO Higgs-sneutrino mass eigenstates are obtained in a generic basis with  $\tilde{\nu}_\alpha \equiv (h_d, \tilde{\nu}_i)$  after the diagonalization of the  $5 \times 5$  mass matrices

$$\mathcal{L} = -\frac{1}{2} \begin{pmatrix} \text{Re} h_u & \text{Re} \tilde{\nu}_\gamma \end{pmatrix} \mathcal{M}_{\text{CPE}}^2 \begin{pmatrix} \text{Re} h_u \\ \text{Re} \tilde{\nu}_\delta \end{pmatrix}, \tag{A.6}$$

$$\mathcal{L} = -\frac{1}{2} \begin{pmatrix} \text{Im} h_u & \text{Im} \tilde{\nu}_\gamma \end{pmatrix} \mathcal{M}_{\text{CPO}}^2 \begin{pmatrix} \text{Im} h_u \\ \text{Im} \tilde{\nu}_\delta \end{pmatrix}, \tag{A.7}$$

---

<sup>8</sup>In ref. [41] the mass matrices are presented in 4-component Dirac notation.

where

$$\mathcal{M}_{\text{CPE}}^2 = \begin{pmatrix} \frac{b_\alpha v_\alpha}{v_u} & -b_\delta \\ -b_\gamma & (m_{\tilde{\nu}}^2)_{\gamma\delta} \end{pmatrix} + \frac{g^2 + g_2^2}{4} \begin{pmatrix} v_u^2 & -v_u v_\delta \\ -v_u v_\gamma & v_\gamma v_\delta \end{pmatrix}, \quad (\text{A.8})$$

$$\mathcal{M}_{\text{CPO}}^2 = \begin{pmatrix} \frac{b_\alpha v_\alpha}{v_u} & b_\delta \\ b_\gamma & (m_{\tilde{\nu}}^2)_{\gamma\delta} \end{pmatrix} + \frac{g^2 + g_2^2}{4} \xi \begin{pmatrix} v_u^2 & -v_u v_\delta \\ -v_u v_\gamma & v_\gamma v_\delta \end{pmatrix}, \quad (\text{A.9})$$

where  $\xi$  is a gauge parameter<sup>9</sup> and

$$(m_{\tilde{\nu}}^2)_{\gamma\delta} \equiv \left[ (m_{\tilde{\mathcal{L}}}^2)_{\gamma\delta} + \mu_\gamma^* \mu_\delta \right] - \frac{(g^2 + g_2^2)}{8} (v_u^2 - |v_\alpha|^2) \delta_{\gamma\delta}. \quad (\text{A.10})$$

Here we have  $|v_\alpha|^2 = v_d^2 + v_i^2$ . The rotation matrices are defined by

$$Z_R^T \mathcal{M}_{\text{CPE}}^2 Z_R = \text{diag} \left[ m_{h^0}^2, m_{H^0}^2, m_{\tilde{\nu}_+^i}^2 \right], \quad i = 1, 2, 3, \quad (\text{A.11})$$

$$Z_A^T \mathcal{M}_{\text{CPO}}^2 Z_A = \text{diag} \left[ m_{G^0}^2, m_{A^0}^2, m_{\tilde{\nu}_-^i}^2 \right], \quad i = 1, 2, 3. \quad (\text{A.12})$$

### Neutrino-neutralino masses

In a general flavour basis, with  $\nu_\beta \equiv (\tilde{h}_d^0, \nu_i)$ , the  $7 \times 7$  neutrino-neutralino mass matrix is given by

$$\mathcal{L} = -\frac{1}{2} \begin{pmatrix} -i\tilde{\mathcal{B}} & -i\tilde{\mathcal{W}}^3 & \tilde{h}_u^0 & \nu_\alpha \end{pmatrix} \mathcal{M}_N \begin{pmatrix} -i\tilde{\mathcal{B}} \\ -i\tilde{\mathcal{W}}^3 \\ \tilde{h}_u^0 \\ \nu_\beta \end{pmatrix}, \quad (\text{A.13})$$

where (at tree level)

$$\mathcal{M}_N = \begin{pmatrix} M_1 & 0 & \frac{1}{2}g v_u & -\frac{1}{2}g v_\beta \\ 0 & M_2 & -\frac{1}{2}g_2 v_u & \frac{1}{2}g_2 v_\beta \\ \frac{1}{2}g v_u & \frac{1}{2}g_2 v_u & 0 & -\mu_\beta \\ -\frac{1}{2}g v_\alpha & \frac{1}{2}g_2 v_\alpha & -\mu_\alpha & 0_{\alpha\beta} \end{pmatrix}. \quad (\text{A.14})$$

The rotation matrix is given by

$$Z_N^T \mathcal{M}_N Z_N = \text{diag}[\tilde{\chi}_a^0, \nu_i], \quad a = 1, 2, 3, 4. \quad i = 1, 2, 3. \quad (\text{A.15})$$

### Charged lepton-chargino masses

The charged lepton-chargino mixing is displayed in the  $5 \times 5$  matrix given below

$$\mathcal{L} = - \left( -i\tilde{\mathcal{W}}^- \quad e_{L_\alpha} \right) \mathcal{M}_C \begin{pmatrix} -i\tilde{\mathcal{W}}^+ \\ \tilde{h}_u^+ \\ e_{R_k}^+ \end{pmatrix} + h.c., \quad (\text{A.16})$$

---

<sup>9</sup> $\xi = 1$  corresponds to the 't Hooft Feynman gauge.

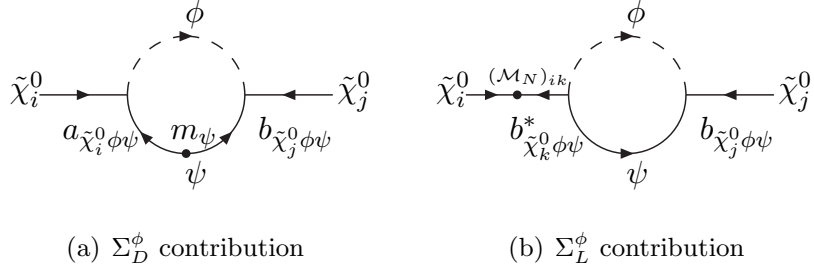


**Figure 5:** One loop self energies: scalar contributions. The  $a$ 's and  $b$ 's represent the vertex Feynman rules that can be found in [25, 41].

where  $e_{L_\alpha} = (\tilde{h}_d^-, e_L^-)$ , and at tree level

$$\mathcal{M}_C = \begin{pmatrix} M_2 & \frac{1}{\sqrt{2}}g_2v_u & 0_k \\ \frac{1}{\sqrt{2}}g_2v_\alpha & \mu_\alpha & \frac{1}{\sqrt{2}}\lambda_{\alpha\beta k}v_\beta \end{pmatrix}. \quad (\text{A.17})$$

The diagonalisation matrices are defined by

$$Z_-^\dagger \mathcal{M}_C Z_+ = \text{diag}[\tilde{\chi}_a^\pm, e_i], \quad a = 1, 2. \quad i = 1, 2, 3. \quad (\text{A.18})$$

## B. One loop self energies of the neutral fermions

For completeness, we list in this appendix the general form of the one loop contributions to the neutral fermion. They can be separated into 4 classes, depending on whether the chirality flip is in the loop or on the external legs, and whether the boson in the loop is a scalar or a vector boson. The complete listing in the RPC limit including the Feynman rules is in [41]. The Feynman rules for the general LNV calculation can be found in [25]. Our expressions are equivalent to the latter, but for the gauge boson contributions, we use the Passarino-Veltman (PV) ‘B’ functions [44] only, and present in a form easier to be compared with [41], which adopts the ‘t Hooft-Feynman gauge ( $\xi = 1$ ).

Recall in the main text that the one loop self energy correction  $\delta\mathcal{M}_{ij}$  takes the form:

$$\delta\mathcal{M}_{ij} = (\Sigma_D)_{ij} - (\mathcal{M}_N)_{ik}(\Sigma_L)_{kj}, \quad (\text{B.1})$$

where  $\Sigma_D$  and  $\Sigma_L$  are the mass and kinetic term corrections respectively.

The contributions from the scalar loops in figure 5 are given by

$$16\pi^2(\Sigma_D^\phi)_{ij}(k^2) = -a_{\tilde{\chi}_i^0\phi\psi}b_{\tilde{\chi}_j^0\phi\psi}m_\psi B_0(k^2, m_\psi^2, m_\phi^2), \quad (\text{B.2})$$

$$16\pi^2(\Sigma_L^\phi)_{kj}(k^2) = b_{\tilde{\chi}_k^0\phi\psi}^*b_{\tilde{\chi}_j^0\phi\psi}B_1(k^2, m_\psi^2, m_\phi^2). \quad (\text{B.3})$$

For the vector boson contributions in figure 6 we have

$$16\pi^2(\Sigma_D^V)_{ij}(k^2) = c_{\tilde{\chi}_i^0\psi}d_{\tilde{\chi}_j^0\psi}m_\psi [4B_0(k^2, m_V^2, m_\psi^2) + \xi B_0(k^2, \xi m_V^2, m_\psi^2) - B_0(k^2, m_V^2, m_\psi^2)], \quad (\text{B.4})$$

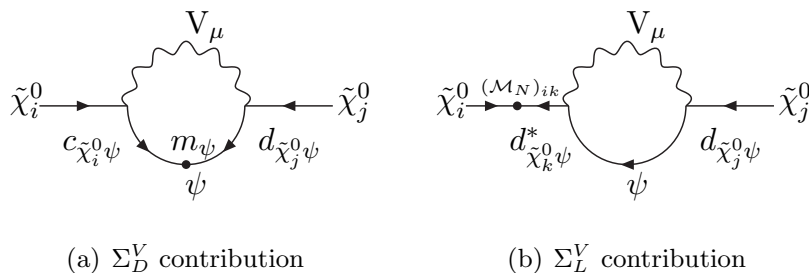


**Figure 6:** One loop self energies: vector boson contributions.

$$\begin{aligned}
 16\pi^2(\Sigma_L^V)_{kj}(k^2) = & d_{\tilde{\chi}_k^0\psi}^* d_{\tilde{\chi}_j^0\psi} [2B_1(k^2, m_\psi^2, m_V^2) \\
 & - \xi B_0(k^2, \xi m_V^2, m_\psi^2) + B_0(k^2, m_V^2, m_\psi^2) \\
 & + \frac{m_\psi^2 - k^2}{m_V^2} (B_1(k^2, \xi m_V^2, m_\psi^2) - B_1(k^2, m_V^2, m_\psi^2))] . \quad (\text{B.5})
 \end{aligned}$$

In the above expressions, the PV functions are defined as in [41]. It should be noted that the definitions of  $B_1$  in [41] and [25] differ by a sign.

### C. Mass insertion approximation in CPE-CPO cancellations

It is well known that loop contributions from CP even (CPE) and CP odd (CPO) scalars tend to cancel each other in many physical processes, because the CPO scalars couple to other fields in the same way as the CPE scalars, apart from the extra  $i$ 's associated with the Feynman rules. In particular, the radiative corrections to the neutrino masses involve strong cancellations among these contributions and may lead to numerical instability. The numerical fluctuation turns out to be irrelevant for the physically interesting LNV parameter space we work in, but as we need to access regions where the light neutrino mass is typically suppressed, this issue needs to be addressed in order to obtain numerically stable results. Another situation where this may be important is when one wishes to consider heavy neutral scalar masses. In this case the numerical fluctuations may be comparable to the physical neutrino masses.

Instead of working directly with the cancellation, we note that in the R-parity conserving limit the cancellation between the CPE and CPO loops is exact. Therefore it is instructive to compute the deviation from this exact cancellation arises from the LNV contributions. We first concentrate on the CPE part. Eq. (3.8) can be diagonalized in two stages, denoted by

$$Z_R = \begin{pmatrix} (Z_H^0)_{2 \times 2} & 0 \\ 0 & (Z_{\tilde{\nu}}^0)_{3 \times 3} \end{pmatrix} \times Z^{\text{MIA}} . \quad (\text{C.1})$$

In the RPC limit,  $Z^{\text{MIA}}$  will be a unit matrix. After the first stage of diagonalization, we get

$$\mathcal{M}_{\text{CPE}}^2 \longrightarrow \begin{pmatrix} (\hat{M}_H^2)_a \delta_{ab} & (Z_H^{0T} \sigma_H Z_{\tilde{\nu}}^0)_{aj} \\ (Z_{\tilde{\nu}}^{0T} \sigma_H^T Z_H^0)_{ib} & (\hat{M}_{\tilde{\nu}}^2)_i \delta_{ij} \end{pmatrix} , \quad (\text{C.2})$$

where  $\{i, j\} = 1 - 3$ ,  $\{a, b\} = 1 - 2$ , and the hatted quantities are diagonal matrices. This matrix is then diagonalized by  $Z^{\text{MIA}}$ , which can be obtained by successive approximations commonly known as mass insertion approximation (MIA). One advantage of performing the diagonalization in these two steps is that in the 't Hooft-Feynman gauge, the  $3 \times 3$  sneutrino part of the CPE and CPO matrices are the same, despite the fact that they also include even powers of lepton-number violating contributions. This means that the terms which contribute to the splittings between the CPE-CPO cancellations are in  $(Z_H^{0T} \sigma_H Z_\nu^0)$ . This procedure also allows us to work in any flavour basis, in which the off diagonal entries  $M_{\tilde{\nu}}^2$  may be large.

Now we can use MIA to obtain the mixing matrix  $Z^{\text{MIA}}$  and the modifications to the eigenvalues. In general, for a symmetric matrix of the form

$$\mathcal{M} = M_\alpha \delta_{\alpha\beta} + \epsilon_{\alpha\beta(\neq\alpha)}, \quad (\text{C.3})$$

where  $\epsilon_{\alpha\beta} \ll M_\alpha$  are matrix perturbations, the mixing matrix  $\mathcal{Z}$  defined by

$$\mathcal{Z}^T \mathcal{M} \mathcal{Z} = \hat{\mathcal{M}} \quad (\text{C.4})$$

can be approximated to second order in  $\epsilon/M$  to be

$$\mathcal{Z}_{\beta\gamma} = \delta_{\beta\gamma} + (\delta Z_\epsilon)_{\beta\gamma} + (\delta Z_{\epsilon^2})_{\beta\gamma} + \mathcal{O}(\epsilon^3/M^3), \quad (\text{C.5})$$

where

$$\begin{aligned} (\delta Z_\epsilon)_{\beta\gamma} &= \epsilon_{\beta\gamma} / (M_\gamma - M_\beta), \\ (\delta Z_{\epsilon^2})_{\beta\gamma} &= -\sum_\rho \epsilon_{\beta\rho} \epsilon_{\rho\gamma} / 2(M_\beta - M_\rho)(M_\gamma - M_\rho) \delta_{\beta\gamma} \\ &\quad + \sum_\rho \epsilon_{\beta\rho} \epsilon_{\rho\gamma(\neq\beta)} / 2(M_\gamma - M_\beta)(M_\gamma - M_\rho), \end{aligned} \quad (\text{C.6})$$

and  $\hat{\mathcal{M}}$  is a diagonal matrix. From here it is easy to obtain an approximate correction to the eigenvalues

$$\delta M_\alpha = \hat{\mathcal{M}}_\alpha - M_\alpha = \sum_\rho \frac{\epsilon_{\alpha\rho} \epsilon_{\rho\alpha}}{M_\alpha - M_\rho}. \quad (\text{C.7})$$

This can be used to obtain the analytic expansion of eq. (3.5) in [25]. In the basis in which we perform our diagonalization of  $\mathcal{M}'_N$ , this is given by

$$\begin{aligned} (\Sigma_D^{\nu\nu})_{ij} &= -\sum_{s=1}^5 \sum_{r=1}^7 \frac{m_{\kappa_r^0}}{(4\pi)^2} \left( \frac{e}{2c_W} Z_{N1r} - \frac{e}{2c_W} Z_{N1r} \right)^2 \\ &\quad \left[ Z_{R(2+i)s} Z_{R(2+j)s} B_0(0, m_{H_s^0}^2, m_{\kappa_r^0}^2) - Z_{A(2+i)s} Z_{A(2+j)s} B_0(0, m_{A_s^0}^2, m_{\kappa_r^0}^2) \right] \end{aligned} \quad (\text{C.8})$$

where  $m_{H_{1,\dots,5}^0}$  and  $m_{A_{1,\dots,5}^0}$  are the CPE and CPO neutral scalars,  $m_{\kappa_{1,\dots,7}^0}$  are the neutral fermions propagating in the loop, and  $Z_R$  and  $Z_A$  are the CPE and CPO scalar mixing matrices respectively. Specifically, we seek an expansion of the expression in square brackets

in eq. (C.8)

$$\begin{aligned}
 & Z_{R(2+i)s} Z_{R(2+j)s} B_0(0, m_{H_s^0}^2, m_{\kappa_r^0}^2) - Z_{A(2+i)s} Z_{A(2+j)s} B_0(0, m_{A_s^0}^2, m_{\kappa_r^0}^2) \\
 & \approx Z_{R(2+i)h} Z_{R(2+j)h} B_0(0, m_{h^0}^2, m_{\kappa_r^0}^2) + Z_{R(2+i)H} Z_{R(2+j)H} B_0(0, m_{H^0}^2, m_{\kappa_r^0}^2) \\
 & \quad - Z_{A(2+i)G} Z_{A(2+j)G} B_0(0, m_{G^0}^2, m_{\kappa_r^0}^2) - Z_{A(2+i)A} Z_{A(2+j)A} B_0(0, m_{A^0}^2, m_{\kappa_r^0}^2) \quad (\text{C.9}) \\
 & \quad + (Z_{R(2+i)\tilde{\nu}_s} Z_{R(2+j)\tilde{\nu}_s} - Z_{A(2+i)\tilde{\nu}_s} Z_{A(2+j)\tilde{\nu}_s}) B_0(0, m_{\tilde{\nu}_s^{\text{CPO}}}^2, m_{\kappa_r^0}^2) \\
 & \quad + (m_{\tilde{\nu}_s^{\text{CPE}}}^2 - m_{\tilde{\nu}_s^{\text{CPO}}}^2) Z_{R(2+i)\tilde{\nu}_s} Z_{R(2+j)\tilde{\nu}_s} C_0(m_{\tilde{\nu}_s^{\text{CPO}}}^2, m_{\tilde{\nu}_s^{\text{CPO}}}^2, m_{\kappa_r^0}^2) \\
 & \quad + \text{higher order terms.}
 \end{aligned}$$

One can then substitute in the results from the MIA to obtain an analytic approximation to  $\mathcal{O}(\sigma^2/M^2)$ . It is rather lengthy to show the full analytic expansion here. We merely note that in the limit of zero sneutrino vevs and no sneutrino mixing, the above expression agrees with eq. (4.10) in [25], apart from the off-diagonal contributions of  $\delta Z_{e^2}$ , which is not included in ref. [25] but is important for our purpose.

## D. Calculation of $l^I \rightarrow l^J \gamma$

In this section we give an explicit calculation of the branching ratio of leptonic FCNC:  $BR(l^I \rightarrow l^J \gamma)$ . For the phase space calculation, 4 component spinor convention as in [68] is used. For the calculation of the loop integrals, 2 component spinor notation is used instead. See the appendix of [25] and references therein for details on the 2 spinor notation calculations.

The effective Lagrangian for decay  $l^I \rightarrow l^J \gamma$  is given by

$$\mathcal{L}_{\text{eff}} = e \bar{l}^J \sigma^{\mu\nu} (\Lambda_L P_L + \Lambda_R P_R) l^I F_{\mu\nu}, \quad (\text{D.1})$$

where  $\sigma^{\mu\nu} = \frac{i}{2}[\gamma^\mu, \gamma^\nu]$ , and  $P_{L/R} = \frac{1}{2}(1 \mp \gamma_5)$ .  $\Lambda_{L(R)}$  are obtained from finite part of one loop diagrams to be described later. In this notation, the matrix element for the process is given by

$$M = 2e \bar{u}_{l^J} \sigma^{\mu\nu} (\Lambda_L P_L + \Lambda_R P_R) u_{l^I} \epsilon_\mu q_\nu, \quad (\text{D.2})$$

where  $u_{l^I}, \bar{u}_{l^J}$  are 4-component Dirac spinors. Summing over final state spins in the matrix element squared, and averaging over the initial  $l^I$  spin, we obtain

$$\begin{aligned}
 K &= \frac{1}{2} \sum_{\epsilon, s_{l^I}, s_{l^J}} |M|^2 \\
 &= 2e^2 \text{Tr} \{ \sigma^{\mu\nu} (\Lambda_L P_L + \Lambda_R P_R) (\not{p}_{l^I} + m_{l^I}) (\Lambda_L^* P_R + \Lambda_R^* P_L) \\
 & \quad \sigma^{\rho\sigma} (\not{p}_{l^J} + m_{l^J}) (-\eta_{\mu\rho}) q_\nu q_\sigma \} \\
 &= 16e^2 (|\Lambda_L|^2 + |\Lambda_R|^2) (q \cdot p_{l^I}) (q \cdot p_{l^J}). \quad (\text{D.3})
 \end{aligned}$$

The decay width of  $l^I \rightarrow l^J \gamma$  is given by the standard formula

$$\begin{aligned}
 \Gamma(l^I \rightarrow l^J \gamma) &= \frac{1}{2m_{l^I}} \int \frac{d^3 p_{l^J}}{(2\pi)^3 2E_{l^J}} \frac{d^3 q}{(2\pi)^3 2E_q} (2\pi)^4 \delta(p_{l^I} - p_{l^J} - q) K \\
 &= \frac{e^2}{4\pi} m_{l^I}^3 (|\Lambda_L|^2 + |\Lambda_R|^2), \quad (\text{D.4})
 \end{aligned}$$



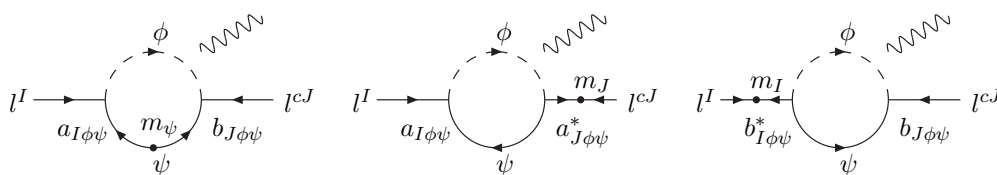


**Figure 7:**  $l^I \rightarrow l^J \gamma$  decay

Using the result  $\Gamma(l^I \rightarrow l^J \bar{\nu}^J \nu^I) = G_F^2 m_l^5 / 192 \pi^3$  (see for example ref. [69]), the branching ratio is then related to  $BR(l^I \rightarrow l^J \bar{\nu}^J \nu^I)$  by

$$BR(l^I \rightarrow l^J \gamma) = \frac{48 \pi^2 e^2}{m_{l^I}^2 G_F^2} (|\Lambda_L|^2 + |\Lambda_R|^2) BR(l^I \rightarrow l^J \bar{\nu}^J \nu^I), \quad (\text{D.5})$$

where the branching ratios  $BR(l^I \rightarrow l^J \bar{\nu}^J \nu^I)$  are given by [38]

$$\begin{aligned} BR(\tau \rightarrow \mu \bar{\nu}^\mu \nu^\tau) &= 0.1736 \pm 0.0005 \\ BR(\tau \rightarrow e \bar{\nu}^e \nu^\tau) &= 0.1784 \pm 0.0005 \\ BR(\mu \rightarrow e \bar{\nu}^e \nu^\mu) &\simeq 1. \end{aligned} \quad (\text{D.6})$$

The calculation of the Wilson coefficients  $\Lambda_L$  and  $\Lambda_R$  can be performed in the 4- or the 2-component formalisms. To compute the loop integrals it probably is slightly easier to use 4 component conventions. On the other hand, the 2 component formalism is more transparent, especially to visualize the helicity flips from the fermion mass insertions. We will use the latter method.

The loop integrals for  $\Lambda_L$  are displayed in figure 7. For a loop with scalar  $\phi$  and fermion  $\psi$ , the  $a_{I\phi\psi}$  couplings correspond to a left-handed, negatively charged lepton  $l^I$  from the SU(2) doublet which flows into the vertex, whereas the  $b_{I\phi\psi}$  couplings correspond to left-handed, positively charged *anti*-lepton  $l^{cI}$  from the SU(2) singlet, again flowing into the vertex. The  $\Lambda_R$  diagrams are similar to the  $\Lambda_L$  ones, and can be obtained by interchanging  $a$  with  $b^*$  and by reversing the helicity flow. Further details can be found in [25] and [56].

The analytic expressions for  $l^I \rightarrow l^J \gamma$  are given by:

$$\begin{aligned} \Lambda_L^{IJ} = \frac{1}{2} \frac{n_c}{(4\pi)^2} \left\{ a_{I\phi\psi} b_{J\phi\psi} m_\psi \left[ \frac{Q_\phi}{m_\phi^2} F_4 \left( \frac{m_\psi^2}{m_\phi^2} \right) - \frac{Q_\psi}{m_\phi^2} F_3 \left( \frac{m_\psi^2}{m_\phi^2} \right) \right] \right. \\ \left. + (a_{I\phi\psi} a_{J\phi\psi}^* m_J + b_{I\phi\psi}^* b_{J\phi\psi} m_I) \left[ \frac{Q_\phi}{m_\phi^2} F_2 \left( \frac{m_\psi^2}{m_\phi^2} \right) - \frac{Q_\psi}{m_\phi^2} F_1 \left( \frac{m_\psi^2}{m_\phi^2} \right) \right] \right\} \end{aligned} \quad (\text{D.7})$$

$$\begin{aligned} \Lambda_R^{IJ} = \frac{1}{2} \frac{n_c}{(4\pi)^2} \left\{ b_{I\phi\psi}^* a_{J\phi\psi}^* m_\psi \left[ \frac{Q_\phi}{m_\phi^2} F_4 \left( \frac{m_\psi^2}{m_\phi^2} \right) - \frac{Q_\psi}{m_\phi^2} F_3 \left( \frac{m_\psi^2}{m_\phi^2} \right) \right] \right. \\ \left. + (b_{I\phi\psi}^* b_{J\phi\psi} m_J + a_{I\phi\psi} a_{J\phi\psi}^* m_I) \left[ \frac{Q_\phi}{m_\phi^2} F_2 \left( \frac{m_\psi^2}{m_\phi^2} \right) - \frac{Q_\psi}{m_\phi^2} F_1 \left( \frac{m_\psi^2}{m_\phi^2} \right) \right] \right\}, \end{aligned} \quad (\text{D.8})$$

where  $Q_\psi$  and  $Q_\phi$  are the electric charges of the scalar and fermion respectively, flowing away from the first vertex in the decay.  $n_c$  is the number of colour in the loop. The loop integrals are given by:

$$\begin{aligned}
 F_1(x) &= \frac{1}{12(1-x)^4} [2 + 3x - 6x^2 + x^3 + 6x \ln x], \\
 F_2(x) &= \frac{1}{12(1-x)^4} [1 - 6x + 3x^2 + 2x^3 - 6x^2 \ln x], \\
 F_3(x) &= \frac{1}{2(1-x)^3} [-3 + 4x - x^2 - 2 \ln x], \\
 F_4(x) &= \frac{1}{2(1-x)^3} [1 - x^2 + 2x \ln x].
 \end{aligned}
 \tag{D.9}$$

Strictly speaking, the above loop integrals are only valid if the external fermion masses are negligible. Contributions from LNV terms typically involve SM fermions in the loop, so the external fermion masses cannot be neglected for a full calculation. However, because the loop scalar remains massive, it is possible to obtain corrections in powers of  $m_l^2/m_\phi^2$ , which are negligible for our purpose.<sup>10</sup> To be more explicit, we use the integral  $F_3$  as an example. The full integral is given by

$$\frac{1}{m_\phi^2} F_3 = \int_0^1 dz \int_0^{1-z} dy \frac{1-z}{z(m_\phi^2 - ym_l^2 - (1-y-z)m_l^2) + (1-z)m_\psi^2}.
 \tag{D.10}$$

Thus the approximation in eq. (D.9) is valid up to  $\sim \mathcal{O}(m_l^2/m_\phi^2)$ . Readers who are interested in applications of the full loop integrals, for example in a supersymmetric theory where the loop scalar mass can be light, may consult [70] for instance.

We have checked explicitly that the above expressions are in agreement with [68] and [58] (in the context of  $b \rightarrow s\gamma$ ).<sup>11</sup> We also checked that the expression for  $(g-2)_\mu$  as well as the numerical results of the SPS benchmarks in the RPC limit agree with [71].

## References

- [1] N. Sakai and T. Yanagida, *Proton decay in a class of supersymmetric grand unified models*, *Nucl. Phys.* **B 197** (1982) 533;  
S. Weinberg, *Supersymmetry at ordinary energies. 1. Masses and conservation laws*, *Phys. Rev.* **D 26** (1982) 287.
- [2] J.L. Goity and M. Sher, *Bounds on  $\Delta B = 1$  couplings in the supersymmetric standard model*, *Phys. Lett.* **B 346** (1995) 69 [*Erratum ibid.* **B 385** (1996) 500] [[hep-ph/9412208](#)];  
A.Y. Smirnov and F. Vissani, *Upper bound on all products of R-parity violating couplings  $\lambda'$  and  $\lambda''$  from proton decay*, *Phys. Lett.* **B 380** (1996) 317 [[hep-ph/9601387](#)]; *Large R-parity violating couplings and grand unification*, *Nucl. Phys.* **B 460** (1996) 37 [[hep-ph/9506416](#)].

---

<sup>10</sup>In fact all the  $x$ 's in eq. (D.9) can be neglected for the LNV loops, apart from a possible top quark in the loop. We include them only for the purpose of comparing with the literature in the R-parity conserving limit, when both the scalar and the fermion in the loop are heavy and so the  $x$ 's cannot be neglected.

<sup>11</sup>The sign of the log term in  $F_4(x)$  as well as the overall signs of the terms involving  $F_1(x)$  and  $F_2(x)$  are different compared to [56].

- [3] H.K. Dreiner, C. Luhn and M. Thormeier, *What is the discrete gauge symmetry of the MSSM?*, *Phys. Rev. D* **73** (2006) 075007 [[hep-ph/0512163](#)].
- [4] L.E. Ibáñez and G.G. Ross, *Discrete gauge symmetry anomalies*, *Phys. Lett. B* **260** (1991) 291.
- [5] R. Barbier et al., *R-parity violating supersymmetry*, *Phys. Rept.* **420** (2005) 1 [[hep-ph/0406039](#)].
- [6] P. Minkowski,  *$\mu \rightarrow e\gamma$  at a rate of one out of  $10^9$  muon decays?*, *Phys. Lett. B* **67** (1977) 421.
- [7] M. Gell-Mann, P. Ramond and R. Slansky, in *Supergravity*, P. van Nieuwenhuizen and D.Z. Freedman eds., North-Holland, Amsterdam The Netherlands (1979).
- [8] W. Buchmüller, L. Covi, K. Hamaguchi, A. Ibarra and T. Yanagida, *Gravitino dark matter in R-parity breaking vacua*, *JHEP* **03** (2007) 037 [[hep-ph/0702184](#)].
- [9] A.S. Joshipura and M. Nowakowski, *'Just so' oscillations in supersymmetric standard model*, *Phys. Rev. D* **51** (1995) 2421 [[hep-ph/9408224](#)].
- [10] M. Nowakowski and A. Pilaftsis, *W and Z boson interactions in supersymmetric models with explicit R-parity violation*, *Nucl. Phys. B* **461** (1996) 19 [[hep-ph/9508271](#)].
- [11] A. Abada and M. Losada, *Constraints on both bilinear and trilinear R-parity violating couplings from neutrino laboratories and astrophysics data*, *Phys. Lett. B* **492** (2000) 310 [[hep-ph/0007041](#)].
- [12] A. Abada, G. Bhattacharyya and M. Losada, *A general analysis with trilinear and bilinear R-parity violating couplings in the light of recent SNO data*, *Phys. Rev. D* **66** (2002) 071701 [[hep-ph/0208009](#)].
- [13] J.C. Romao, M.A. Diaz, M. Hirsch, W. Porod and J.W.F. Valle, *A supersymmetric solution to the solar and atmospheric neutrino problems*, *Phys. Rev. D* **61** (2000) 071703 [[hep-ph/9907499](#)].
- [14] M. Hirsch, M.A. Diaz, W. Porod, J.C. Romao and J.W.F. Valle, *Neutrino masses and mixings from supersymmetry with bilinear R-parity violation: a theory for solar and atmospheric neutrino oscillations*, *Phys. Rev. D* **62** (2000) 113008 [*Erratum* *ibid.* **D 65** (2002) 119901] [[hep-ph/0004115](#)].
- [15] M.A. Diaz, M. Hirsch, W. Porod, J.C. Romao and J.W.F. Valle, *Solar neutrino masses and mixing from bilinear R-parity broken supersymmetry: analytical versus numerical results*, *Phys. Rev. D* **68** (2003) 013009 [*Erratum* *ibid.* **D 71** (2005) 059904] [[hep-ph/0302021](#)].
- [16] A. Abada, S. Davidson and M. Losada, *Neutrino masses and mixings in the MSSM with soft bilinear  $R_p$  violation*, *Phys. Rev. D* **65** (2002) 075010 [[hep-ph/0111332](#)].
- [17] D.E. Kaplan and A.E. Nelson, *Solar and atmospheric neutrino oscillations from bilinear R-parity violation*, *JHEP* **01** (2000) 033 [[hep-ph/9901254](#)].
- [18] H.-P. Nilles and N. Polonsky, *Supersymmetric neutrino masses, R-symmetries and the generalized  $\mu$  problem*, *Nucl. Phys. B* **484** (1997) 33 [[hep-ph/9606388](#)].
- [19] Y. Grossman and S. Rakshit, *Neutrino masses in R-parity violating supersymmetric models*, *Phys. Rev. D* **69** (2004) 093002 [[hep-ph/0311310](#)].
- [20] Y. Grossman and H.E. Haber, *Sneutrino mixing phenomena*, *Phys. Rev. Lett.* **78** (1997) 3438 [[hep-ph/9702421](#)].

- [21] Y. Grossman and H.E. Haber, *(S)neutrino properties in R-parity violating supersymmetry. I: CP-conserving phenomena*, *Phys. Rev. D* **59** (1999) 093008 [[hep-ph/9810536](#)].
- [22] S. Davidson and M. Losada, *Neutrino masses in the  $R_p$  violating MSSM*, *JHEP* **05** (2000) 021 [[hep-ph/0005080](#)].
- [23] A.S. Joshipura and S.K. VemPati, *Sneutrino vacuum expectation values and neutrino anomalies through trilinear R-parity violation*, *Phys. Rev. D* **60** (1999) 111303 [[hep-ph/9903435](#)].
- [24] S. Davidson and M. Losada, *Basis independent neutrino masses in the  $R(p)$  violating MSSM*, *Phys. Rev. D* **65** (2002) 075025 [[hep-ph/0010325](#)].
- [25] A. Dedes, S. Rimmer and J. Rosiek, *Neutrino masses in the lepton number violating MSSM*, *JHEP* **08** (2006) 005 [[hep-ph/0603225](#)].
- [26] P.F. Harrison, D.H. Perkins and W.G. Scott, *Tri-bimaximal mixing and the neutrino oscillation data*, *Phys. Lett. B* **530** (2002) 167 [[hep-ph/0202074](#)].
- [27] B.C. Allanach, A. Dedes and H.K. Dreiner, *Bounds on R-parity violating couplings at the weak scale and at the GUT scale*, *Phys. Rev. D* **60** (1999) 075014 [[hep-ph/9906209](#)].
- [28] B.C. Allanach, A. Dedes and H.K. Dreiner, *The R parity violating minimal supergravity model*, *Phys. Rev. D* **69** (2004) 115002 [*Erratum ibid.* **D 72** (2005) 079902] [[hep-ph/0309196](#)].
- [29] A. Datta, J.P. Saha, A. Kundu and A. Samanta, *Rare weak decays and direct lepton number violating signals in a minimal R-parity violating model of neutrino mass*, *Phys. Rev. D* **72** (2005) 055007 [[hep-ph/0507311](#)].
- [30] R. Hempfling, *Neutrino masses and mixing angles in SUSY-GUT theories with explicit R-parity breaking*, *Nucl. Phys. B* **478** (1996) 3 [[hep-ph/9511288](#)].
- [31] V.D. Barger, R.J.N. Phillips and K. Whisnant, *Long wave length oscillations and the GALLEX solar neutrino signal*, *Phys. Rev. Lett.* **69** (1992) 3135 [[hep-ph/9207257](#)].
- [32] KAMLAND collaboration, K. Eguchi et al., *First results from KamLAND: evidence for reactor anti-neutrino disappearance*, *Phys. Rev. Lett.* **90** (2003) 021802 [[hep-ex/0212021](#)].
- [33] E.J. Chun, S.K. Kang, C.W. Kim and U.W. Lee, *Supersymmetric neutrino masses and mixing with R-parity violation*, *Nucl. Phys. B* **544** (1999) 89 [[hep-ph/9807327](#)].
- [34] B. de Carlos and P.L. White, *R-parity violation effects through soft supersymmetry breaking terms and the renormalisation group*, *Phys. Rev. D* **54** (1996) 3427 [[hep-ph/9602381](#)].
- [35] L. Wolfenstein, *Neutrino oscillations in matter*, *Phys. Rev. D* **17** (1978) 2369; *Neutrino oscillations and stellar collapse*, *Phys. Rev. D* **20** (1979) 2634; S.P. Mikheev and A.Y. Smirnov, *Resonance enhancement of oscillations in matter and solar neutrino spectroscopy*, *Sov. J. Nucl. Phys.* **42** (1985) 913 [*Yad. Fiz.* **42** (1985) 1441]; *Resonant amplification of neutrino oscillations in matter and solar neutrino spectroscopy*, *Nuovo Cim.* **C9** (1986) 17.
- [36] M.C. Gonzalez-Garcia and M. Maltoni, *Phenomenology with massive neutrinos*, [arXiv:0704.1800](#).

- [37] Z. Maki, M. Nakagawa and S. Sakata, *Remarks on the unified model of elementary particles*, *Prog. Theor. Phys.* **28** (1962) 870;  
B. Pontecorvo, *Neutrino experiments and the question of leptonic-charge conservation*, *Sov. Phys. JETP* **26** (1968) 984 [*Zh. Eksp. Teor. Fiz.* **53** (1967) 1717].
- [38] PARTICLE DATA GROUP collaboration, W.M. Yao et al., *Review of particle physics*, *J. Phys.* **G 33** (2006) 1.
- [39] S.P. Martin and M.T. Vaughn, *Two loop renormalization group equations for soft supersymmetry breaking couplings*, *Phys. Rev.* **D 50** (1994) 2282 [[hep-ph/9311340](#)].
- [40] R. Barbieri, L.J. Hall and A. Strumia, *Violations of lepton flavor and CP in supersymmetric unified theories*, *Nucl. Phys.* **B 445** (1995) 219 [[hep-ph/9501334](#)].
- [41] D.M. Pierce, J.A. Bagger, K.T. Matchev and R.-j. Zhang, *Precision corrections in the minimal supersymmetric standard model*, *Nucl. Phys.* **B 491** (1997) 3 [[hep-ph/9606211](#)].
- [42] E. Nardi, *Renormalization group induced neutrino masses in supersymmetry without R-parity*, *Phys. Rev.* **D 55** (1997) 5772 [[hep-ph/9610540](#)].
- [43] B.C. Allanach et al., *The snowmass points and slopes: benchmarks for SUSY searches*, *Eur. Phys. J.* **C 25** (2002) 113 [*eConf C010630* (2001) P125] [[hep-ph/0202233](#)].
- [44] G. 't Hooft and M. Veltman, *Scalar one-loop integrals*, *Nucl. Phys.* **B 153** (1979) 365;  
G. Passarino and M. Veltman, *One-loop corrections for  $e^+e^-$  annihilation into  $\mu^+\mu^-$  in the Weinberg model*, *Nucl. Phys.* **B 160** (1979) 151.
- [45] B.C. Allanach, *SOFTSUSY 2.0: a C++ program for calculating supersymmetric spectra*, *Comput. Phys. Commun.* **143** (2002) 305 [[hep-ph/0104145](#)].
- [46] CDF collaboration, J.F. Arguin et al., *Combination of CDF and D0 results on the top-quark mass*, [hep-ex/0507091](#).
- [47] F. James, *MINUIT minimization package reference manual version 94.1*,  
<http://wwwasdoc.web.cern.ch/wwwasdoc/WWW/minuit/minmain/minmain.html>.
- [48] M. Fukugita, K. Ichikawa, M. Kawasaki and O. Lahav, *Limit on the neutrino mass from the WMAP three year data*, *Phys. Rev.* **D 74** (2006) 027302 [[astro-ph/0605362](#)].
- [49] MEGA collaboration, M. Ahmed et al., *Search for the lepton-family-number nonconserving decay  $\mu^+ \rightarrow e^+\gamma$* , *Phys. Rev.* **D 65** (2002) 112002 [[hep-ex/0111030](#)].
- [50] BABAR collaboration, B. Aubert et al., *Search for lepton flavor violation in the decay  $\tau^\pm \rightarrow e^\pm\gamma$* , *Phys. Rev. Lett.* **96** (2006) 041801 [[hep-ex/0508012](#)].
- [51] BABAR collaboration, B. Aubert et al., *Search for lepton flavor violation in the decay  $\tau \rightarrow \mu\gamma$* , *Phys. Rev. Lett.* **95** (2005) 041802 [[hep-ex/0502032](#)].
- [52] *Search for the rare decays  $B_{s(d)} \rightarrow \mu^+\mu^-$* ,  
<http://www-cdf.fnal.gov/physics/new/bottom/060316.blessed-bsmumu3/>.
- [53] B.C. Allanach, M.A. Bernhardt, H.K. Dreiner, C.H. Kom and P. Richardson, *Mass spectrum in R-parity violating mSUGRA and benchmark points*, *Phys. Rev.* **D 75** (2007) 035002 [[hep-ph/0609263](#)].
- [54] HEAVY FLAVOR AVERAGING GROUP (HFAG) collaboration, E. Barberio et al., *Averages of b-hadron properties at the end of 2005*, [hep-ex/0603003](#).

- [55] P. Gambino and M. Misiak, *Quark mass effects in  $\bar{B} \rightarrow X_s \gamma$* , *Nucl. Phys.* **B 611** (2001) 338 [hep-ph/0104034];  
A.J. Buras, A. Czarnecki, M. Misiak and J. Urban, *Completing the NLO QCD calculation of  $\bar{B} \rightarrow X_s \gamma$* , *Nucl. Phys.* **B 631** (2002) 219 [hep-ph/0203135].
- [56] S. Rimmer,  *$l \rightarrow l' \gamma$  in the lepton number violating MSSM*, hep-ph/0610406.
- [57] J.-H. Jang, J.K. Kim and J.S. Lee, *Constraints on the R-parity and lepton flavor violating couplings from  $B_0$  decays to two charged leptons*, *Phys. Rev.* **D 55** (1997) 7296 [hep-ph/9701283].
- [58] T. Besmer and A. Steffen, *R-parity violation and the decay  $b \rightarrow s \gamma$* , *Phys. Rev.* **D 63** (2001) 055007 [hep-ph/0004067].
- [59] M. Misiak, S. Pokorski and J. Rosiek, *Supersymmetry and FCNC effects*, *Adv. Ser. Direct. High Energy Phys.* **15** (1998) 795 [hep-ph/9703442].
- [60] F. Borzumati and J.S. Lee, *Novel constraints on  $\Delta_L = 1$  interactions from neutrino masses*, *Phys. Rev.* **D 66** (2002) 115012 [hep-ph/0207184].
- [61] J.R. Ellis, K. Enqvist, D.V. Nanopoulos and F. Zwirner, *Observables in low-energy superstring models*, *Mod. Phys. Lett.* **A 1** (1986) 57.
- [62] H. Abe, T. Kobayashi and Y. Omura, *Relaxed fine-tuning in models with non-universal gaugino masses*, *Phys. Rev.* **D 76** (2007) 015002 [hep-ph/0703044].
- [63] H. Baer and X. Tata, *Weak scale supersymmetry: from superfields to scattering events*, Cambridge University Press, Cambridge U.K..
- [64] F.E. Paige, S.D. Protopopescu, H. Baer and X. Tata, *ISAJET 7.69: a Monte Carlo event generator for  $pp$ ,  $\bar{p}p$  and  $e^+e^-$  reactions*, hep-ph/0312045.
- [65] N. Nimai Singh, H. Zeen Devi and M. Patgiri, *Phenomenology of neutrino mass matrices obeying  $\mu$ - $\tau$  reflection symmetry*, arXiv:0707.2713.
- [66] L.E. Ibáñez and G.G. Ross, *Fermion masses and mixing angles from gauge symmetries*, *Phys. Lett.* **B 332** (1994) 100 [hep-ph/9403338].
- [67] H.K. Dreiner, J. Soo Kim and M. Thormeier, *A simple baryon triality model for neutrino masses*, arXiv:0711.4315.
- [68] A. Dedes, H.E. Haber and J. Rosiek, *Seesaw mechanism in the sneutrino sector and its consequences*, *JHEP* **11** (2007) 059 [arXiv:0707.3718].
- [69] T.P. Cheng and L.F. Li, *Gauge theory of elementary particle physics*, Clarendon press, Oxford U.K. (1988).
- [70] T. Ibrahim and P. Nath, *Effects of large CP-violating phases on  $g_\mu - 2$  in MSSM*, *Phys. Rev.* **D 62** (2000) 015004 [hep-ph/9908443].
- [71] D. Stöckinger, *The muon magnetic moment and supersymmetry*, *J. Phys.* **G 34** (2007) R45 [hep-ph/0609168].